

AD-757 234

COMBUSTION TRANSIENTS OF SOLID PROPELLANTS

Norman W. Ryan, et al

Utah University

Prepared for:

Air Force Office of Scientific Research

28 February 1973

DISTRIBUTED BY:

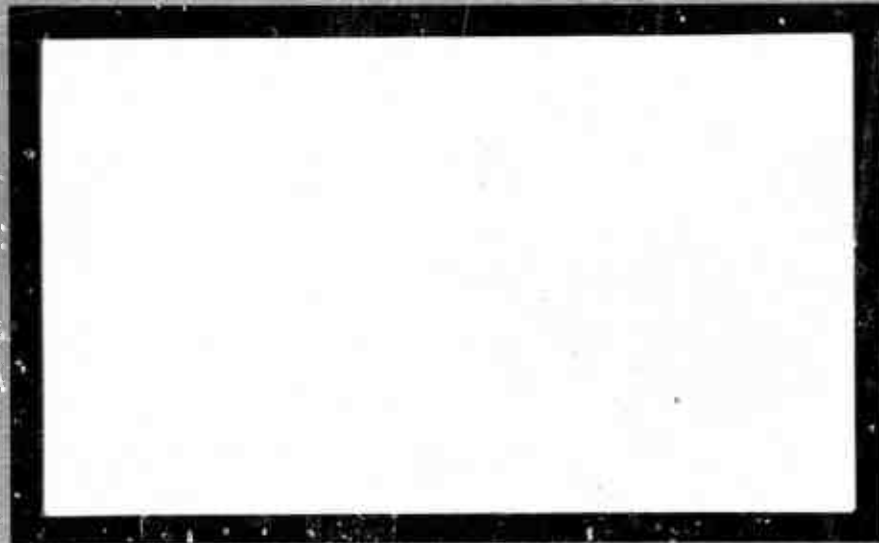
NTIS

National Technical Information Service
U. S. DEPARTMENT OF COMMERCE
5285 Port Royal Road, Springfield Va. 22151

AFOSR - TR - 73 - 0437

AD757234

University of Utah
Department of Chemical Engineering



Salt Lake City, Utah



Approved for public release;
distribution unlimited.

R 70

UNCLASSIFIED

Security Classification

| DOCUMENT CONTROL DATA - R & D | | |
|---|--|---|
| <i>(Security classification of title, body of abstract and indexing annotation must be entered when the overall report is classified)</i> | | |
| 1. ORIGINATING ACTIVITY (Corporate author) UNIVERSITY OF UTAH DEPARTMENT OF CHEMICAL ENGINEERING SALT LAKE CITY, UTAH 84112 | | 2a. REPORT SECURITY CLASSIFICATION UNCLASSIFIED |
| | | 2b. GROUP |
| 3. REPORT TITLE COMBUSTION TRANSIENTS OF SOLID PROPELLANTS | | |
| 4. DESCRIPTIVE NOTES (Type of report and inclusive dates) Scientific Final | | |
| 5. AUTHOR(S) (First name, middle initial, last name) NORMAN W RYAN ALVA D BAER | | |
| 6. REPORT DATE 28 Feb 1973 | 7a. TOTAL NO OF PAGES 68 70 | 7b. NO. OF REFS 20 |
| 8a. CONTRACT OR GRANT NO AFOSR-69-1656 | 9a. ORIGINATOR'S REPORT NUMBER(S) | |
| b. PROJECT NO. 9711-01 | | |
| c. 61102F | 9b. OTHER REPORT NO(S) (Any other numbers that may be assigned this report) | |
| d. 681307 | AFOSR - TR - 73 - 0437 | |
| 10. DISTRIBUTION STATEMENT Approved for public release; distribution unlimited. | | |
| 11. SUPPLEMENTARY NOTES TECH, OTHER | | 12. SPONSORING MILITARY ACTIVITY AF Office of Scientific Research (NAE) 1400 Wilson Blvd. Arlington, Va. 22209 |
| 13. ABSTRACT Under the subject grant, several distinct but related studies of the combustion dynamics of solid propellants were undertaken. As the results of most of the work have been presented previously, this report is largely a restatement of conclusions, with reference to previous publications for details. The areas of study reported are an evaluation of the hot-wire-ignition method for characterizing propellants; the development and study of a gas-fueled analog of the solid-propellant T-burner; a study of low frequency (L*) combustion of L* during a test; a study of high frequency acoustic instability of solid propellants, both a T-burner and a radial-mode, radial-flow burner being used with the same propellants systems; the development and evaluation of a technique for measuring the solid-propellant response function to external energy perturbations at the burning surface; the measurement and evaluation of transient temperatures of propellant flames during rapid depressurization; and a detailed characterization of the low-pressure-combustion phenomena for several different solid propellants including studies of the low-pressure deflagration limit, the electrical conductance near the surface, the extinguishment requirements, and spontaneous reignition. | | |

DD FORM 1473
1 NOV 65

UNCLASSIFIED

Security Classification

UNIVERSITY OF UTAH
DEPARTMENT OF CHEMICAL ENGINEERING

Final Report

COMBUSTION TRANSIENTS OF SOLID PROPELLANTS

AFOSR Grant 69-1656

28 February 1973



Work performed under sponsorship of the Combustion Energetics
Division of the Air Force Office of Scientific Research.

Report prepared by A. D. BAER

and N. W. RYAN



Abstract

Under the subject grant, several distinct but related studies of the combustion dynamics of solid propellants were undertaken. As the results of most of the work have been presented previously, this report is largely a restatement of conclusions, with reference to previous publications for details.

The areas of study reported are an evaluation of the hot-wire-ignition method for characterizing propellants; the development and study of a gas-fueled analog of the solid-propellant T-burner; a study of low-frequency (L^*) combustion instability, in which study the burner used permits both increase and decrease of L^* during a test; a study of high frequency acoustic instability of solid propellants, both a T-burner and a radial-mode, radial-flow burner being used with the same propellant systems; the development and evaluation of a technique for measuring the solid-propellant response function to external energy perturbations at the burning surface; the measurement and evaluation of transient temperatures of propellant flames during rapid depressurization; and a detailed characterization of the low-pressure-combustion phenomena for several different solid propellants including studies of the low-pressure deflagration limit, the electrical conductance near the surface, the extinguishment requirements, and spontaneous reignition.

TABLE OF CONTENTS

| | |
|--|----|
| Abstract | 11 |
| I. Introduction | 1 |
| II. Hot-wire Ignition | 2 |
| III. Low Frequency Combustion Instability | 3 |
| IV. Acoustic Instability in a Radial Mode Burner | 5 |
| V. Gas-fired T-burner Studies | 9 |
| VI. Propellant Response to Thermal Radiation | 12 |
| VII. Propellant Response to Electrical Dissipation at the Surface | 16 |
| VIII. Propellant Flame Temperatures during Depressurization . . . | 20 |
| IX. Propellant Extinguishment and Burning at Low Pressures . . | 25 |
| Summary | 33 |
| Appendix A - Figures | 36 |
| Appendix B - References | 64 |

I. INTRODUCTION

During the four-year period of this grant, research efforts have encompassed nearly all of the areas of combustion dynamics of solid propellants. Work was completed on the evaluation and use of the hot-wire ignition technique for characterizing solid propellant ignition. Extensive experiments were conducted and a theoretically based interpretation of the experimental results was made of low frequency (L^*) combustion instability were explored by use of a gas-fired T-burner. The very-high-frequency combustion-instability region was studied by use of a radial-mode burner, and the problem of translation of instability data from a conventional T-burner to the radial mode configuration were treated. A technique was developed which employed the transient, combustion-recoil from burning strands to characterize the stability characteristics of propellants and to evaluate current instability models. The extinguishment requirements of composite propellants were studied by use of a rarefaction tube, and an extensive study of burning and extinguishment at low pressure was made.

A total of six Ph D candidates and two M. S. candidates have been supported by this grant. In general, each student has been responsible for an area of work, and in most cases the individual projects described below represent the experimental efforts of a junior investigator. Only projects which have been essentially completed are reported here. Work which was started late in the period of this grant and which is being continued under Grant AFOSR 73-2470 is not discussed.

In most cases, this work has been previously presented in technical

reports and journal articles. The presentations in the following paragraphs are intended to present a summary of the overall research effort and to present the highlights and the principal conclusions of the work. Although the projects are closely related, each principal effort is presented as a separate section of this report. For the sake of consistency, all figures and references are assembled at the end of the text.

II. HOT-WIRE IGNITION

Ignition by imbedded, electrically heated wires is one of the oldest techniques for characterizing propellant ignition. It has not been widely used mainly because it is difficult to measure short ignition times accurately when the heated surface is not in view. During preliminary tests, in which the composite propellant was cast around fine Nichrome wires, it was discovered that accurate detection of ignition could be achieved by observing irregularities in the electrical current through the wires. These irregularities resulted from the formation of a high density, partially ionized gas around the wires. Ignition times accurate to about ± 1 msec were measured. Two papers were prepared [1,2], under this grant, evaluating the hot-wire method for characterizing the high-pressure, pressure-independent ignition processes of several composite propellants. The hot-wire ignition technique was shown to be a convenient and accurate method for evaluating the parameters of the critical ignition reactions. Tests with fine, 25-micron diameter wires have produced evidence of a 10-20 kcal/g-mole-activation energy, distributed reaction which supplements the effect of the 30 kcal/g-mole

interfacial reaction. Figure 1 shows evidence of this effect. The two-reaction model (interface and distributed) with a single set of parameters reproduces experimental ignition data from all hot-wire tests on several composite propellants.

Except when the effects of the distributed reactions were exaggerated by use of very fine wires or very long ignition times, an accurate representation of all the hot-wire-ignition data on AP-PBAA composites was obtained by a model employing the same surface-reaction parameters previously used to characterize ignition by radiant-heat fluxes [3], high convective heat fluxes [4,5] and low convective heat fluxes [6]. Figure 2 shows the comparison between experiment and theory for over a 10^7 range of dimensionless ignition times. These data are about equally well represented by a model which involves a distributed phase reaction with an activation energy of 20 kcal/g-mole, but the exposed surface data are not well represented by such a model.

III. LOW FREQUENCY COMBUSTION INSTABILITY

Both in volume and accuracy, data on non-acoustic combustion instability of solid propellants have been inadequate to permit evaluating hypotheses concerning the nature of the phenomenon. The first task of this study was devising and using an experiment in which accurate data could be obtained. The principal experiment used for this purpose was a burner of small-volume with an end burning configuration. The stability or instability was inferred from chamber pressure just after the ignition transient, and the data obtained from this type of tests were excellent. Six propellants were studied, and the effect of burner

diameter on the data was evaluated. The results obtained for 1.0, 1.25, and 1.5 inch diameters were in agreement, indicating that small burners are satisfactory for such studies. A detailed technical report describing this work has been prepared [7].

In the conventional small-volume burner used for low frequency tests, L^* increases during burning, instability being most likely at the start of the test. It was very important to determine whether instability would occur at the same value of L^* if L^* were decreasing, initial burning being stable. It was also important to establish that the ignition transient did not trigger the instability because the proposed theory assumes that oscillations are self-excited. A modified L^* burner was constructed with a movable nozzle section that could be advanced toward the surface of the end-burning grain. An exploded view of this burner is shown in Figure 3. With the modified L^* burner it was possible to decrease the L^* during the test and to approach the instability region from the stable regime. The data obtained from the modified L^* burner agreed with the conventional L^* burner results. Figure 4 presents typical results for a catalyzed AP composite.

A theory proposed in this study was an extensive mathematical model in which the most significant original feature is the assumption that the gas phase is a stirred reactor. A set of eight equations was required to define the combustion process. Perturbation analysis was employed to linearize this set of equations. A complete solution yielding degree of instability was not attempted. A partial solution, yielding stability limits was obtained [7]. From this solution, it was possible to evaluate numerically the relationships between pressure and the frequency of the

oscillations and the critical L^* for a given set of propellant and burner parameters. Not all of the propellant parameters are known; values of most have been reported or can easily be calculated, and the remaining ones can be reasonably estimated for the propellants studied. Figure 4 shows a comparison between the experimental results and the theoretical predictions. Because the magnitude of some of the parameters of the theory has been estimated such agreement is not real evidence of the validity of the theory.

The experimental data demonstrated that good quantitative data could be obtained from stable-unstable type of tests. The modified L^* -motor provided an additional experimental tool for obtaining non-acoustic instability data; propellant diameter had no effect on non-acoustic combustion instability when the data are presented in terms of pressure versus L^* . Finally, it appears that the modular model proposed in this investigation provided a theoretical basis for explaining the experimental observations.

IV. ACOUSTIC INSTABILITY IN A RADIAL MODE BURNER

One of the important unsolved problems of solid-propellant-combustion dynamics is the application of acoustic-instability theory to an actual motor situation. The important propellant parameters of such theories can supposedly be supplied from laboratory test devices such as the T-burner; however, attempts to quantitatively explain motor instability by use of T-burner-derived parameters have not been successful. The work described here was in part motivated by recognition of the extreme difficulties in applying data from the simple one-dimensional

T-burner to solution of the multi-dimensional motor problem. There was an obvious need for a test device intermediate in complexity between the T-burner and a small-scale engine; translation of T-burner derived parameters to the conditions of the intermediate device would serve as a test of current theories. This exercise would hopefully also suggest the reasons for failure to be able to apply the theories to the motor situation. Reference [8] is a detailed presentation of this development of the intermediate device, a radial-flow, radial-mode burner, and the following paragraphs summarize the important results of this study.

The measure of tendency to acoustic instability is the measured growth of the acoustic pressure amplitude,

$$\alpha_g = d \ln p/dt,$$

corrected for losses,

$$\alpha = \alpha_g - \alpha_d,$$

where α_d is intrinsically negative. Two methods were used to obtain α . In the growth-and-decay method, it is assumed that losses are the same at the end of the test as at the beginning, and α_d is measured just after burn-out [9]. The other technique is the variable-area method [9].

Historically, the two methods have not yielded the same values of α_d for a given propellant, an observation reconfirmed in this study. Therefore, while a given experimenter using either of the methods may obtain a valuable comparison of propellants, there remains some doubt as to whether his α values are the proper ones for calculating an admittance function which is a property of a propellant. It was in part this doubt, as an aspect of general ignorance about the magnitudes of the several kinds of acoustic losses, which also motivated experiments with

a burner in which the radial, rather than longitudinal, modes of oscillation are excited. Losses in T-burner and radial-burners are related to geometrical parameters and frequency in different ways.

The radial burner shown in Figure 5 consists of a short cylindrical section, 1 or 2 inches long, 6 inches in diameter, closed at the ends by flat flanges. One flange contains six vents symmetrically disposed at the radial position of the pressure node of the first-radial mode of oscillation. Six, three or two vents were used for any given firing. A strip of propellant, 0.22 or 0.5-inch web thickness, was bonded to the cylindrical wall, and pressure transducers were mounted in that wall. In some tests a center post was used, sometimes inert, sometimes of propellant. Supplemental tests were made with the same propellants in a 1 1/2 inch-diameter T-burner. All firings were made with choked flow in the vents.

General observations on tests with the radial burner are as follows. Tests with two transducers were designed to detect the presence of mixed modes or the rotation of the tangential (sloshing) modes (when present). Neither was detected in preliminary tests. However, occasionally the first radial (1R) and the first tangential (1T) modes were present simultaneously. The second tangential (2T) mode was sometimes observed.

The 1T mode was found dominant unless surfaces to fix the velocity node and vents are distributed in a way to suppress it and favor the 1R mode such as use of the six vents. Replacing the propellant center post with an inert center post when six vents are used favors the 1T mode; though growth is usually still 1R, decay is more likely to be 1T.

In order that T-burner and radial burner results may be analyzed to infer something about loss mechanisms, there must be reasonable agreement between expected and realized values of α . Strictly speaking,

with data of this study, comparison could properly be made (matching frequency and pressure) only between the 1L mode of the T-burner (for shortest tube, 3.5 to 4.3 kHz) and the 1T mode of the radial-burner (3.0 to 4.0 kHz). Figures 6 and 7 show growth and decay results from an AP-PBAA composite. According to theory [8] α from 1L in the T-burner should be 2.4 times α for 1T in the radial burner. Actually, as inferred from experimental data, the factor was 0.9.

Attempts to rationalize the discrepancy have not been successful. On the other hand, the results actually obtained may be meaningful. It is conceivable that the measured α_d may adequately reflect losses in the T-burner (1L mode) but not in the radial burner (1T) mode. There may be additional losses, absent during post-burn-out decay, due to acoustic velocity-burning rate coupling at those parts of the burning surface exposed to acoustic cross-flow.

There is the disturbing observation that the measured α_d has the same value, $-33 \pm 4 \text{ sec}^{-1}$, for both burners and all pressures, frequencies, and oscillation modes tested. It was measured from oscillations decaying during the period of falling mean pressure just after burn-out in the nozzled chamber. This variation of the growth-and-decay method has never been tested against the conventional version, in which mean pressure is held constant. However, there is no a priori reason why it should not serve as well.

A cursory look was taken at the proposition that at the frequencies of interest (7.5 to 9.5 kHz in the 1R mode), the thermal wave in the propellant is not a capacitive element of the oscillating system, the role being played, instead, by gas-phase chemistry. The correlation shown in Figure 8 of the pseudo-steady state oscillating pressure supports this

proposition. An acoustic energy balance is written for the flame zone, the generation term being the perturbed rate of sensible energy release by chemical reaction times an efficiency of conversion to acoustic energy. Kinetic, quasi-equilibrium, and energy equations in simple forms are perturbed to inter-relate pressure, temperature, and conversion perturbations, and an expression for the admittance function is obtained.

Whatever procedure is used in the analysis, the result will show that the admittance function is proportional to the efficiency of energy conversion in the gas phase. Unless this new parameter can be independently determined, the expression has no predictive value. Nevertheless, if the concept is valid, the nature of the efficiency factor can be inferred from experimental data. From data for the 1L mode in the T-burner, for the conditions employed, it was found that the efficiency is proportional to $P^{1-n} f^{-1}$, where P is mean pressure and n the exponent on the steady-state burning law. The frequency dependence is in the right direction, but it is probably too strong to be explained by chemical kinetic effects.

Although there are many more questions raised by this work than answers supplied, it appears that correspondence between T-burner and the radial-mode burner parameters cannot be obtained by use of current theoretical results.

V. GAS-FIRED T-BURNER STUDIES

This study required the development and use of a new experimental device--the gas-fired T-burner. Patterned after the solid propellant T-burner, the gas burner represents a significant improvement in flexibility and controllability. Its behavior is strikingly similar

to that of the solid-propellant T-burner, primarily in its tendency to oscillate in its fundamental longitudinal mode with exponentially increasing amplitude. Reference [10] presents a detailed report of this work and references [11, 12] are papers based upon this study.

Figure 9 shows an exploded view of the 1 1/2 inch diameter gas-fired burner used in these tests. Premixed combustible mixtures entered a plenum chamber at the end opposite to a stainless steel frit. Flow rates through the frit were set to produce energy release rates in the gaseous flame comparable to the rates of solid-propellant flames and high enough to prevent transfer of acoustical disturbances in the combustion chamber into the plenum chamber and gas feed systems. Exhaust of the combustion products was through a carbon nozzle and into the atmosphere. Ignition of the mixture in the combustion chamber was achieved by means of an automotive spark plug, and the exponential growth of acoustic oscillations was observed soon after ignition. The rate of growth of the acoustic pressure was normally slow enough to permit measurement of the growth constants, α , at 0.1 to 0.15 seconds after ignition during a period of essentially constant pressure.

Exponential growth constants have been measured and correlated with composition under a wider variety of run conditions than can be attained with solid propellants. By careful attention to detail, the effects of small variation in run conditions were ascertained with confidence. Data showing the effects of mass-flow rate, frequency, and inert-gas dilution on a α -vs. the equivalence ratio, ϕ , relationship were obtained. Figure 10 shows values of the measured growth constants as a function of ϕ for air and nitrogen-diluted air-methane mixtures. Growth constants are seen to

be strongly dependent on the fuel-oxidant ratio and exhibit maxima near the maximum temperature composition, which would be expected. The maximum near the fuel-lean ignition limit, was completely unexpected.

From these results, a fairly strong inference can be drawn, implicating gas-phase combustion kinetics as an important driving force in acoustic instability. This inference is supported by a consideration of the characteristics of the gas-fired-burner frit. The assumed response of the solid-propellant surface to an increasing pressure perturbation is to increase the rate of gasification of solid i.e., the response function of an acoustic instability theory should be positive. In the case of the response of the frit, it is likely that the increasing pressure perturbation would reduce the rate of fuel entering the gaseous region, i.e. the response function would be negative. It thus appears that the acoustic instability of the gas-fired burner should best be described in terms of gas phase energy release. The important question is whether the solid propellant response at high frequencies should also be described in the same way.

Because of the unusually good reproducibility in growth constants obtained from the final burner configurations, it was possible to study the effects of various hold-off or oscillation damping devices. By far the most effective technique was to employ a tuned, dissipative Helmholtz cavity at the pressure anti-node opposite the combustion zone. High linear losses were obtained by use of an opening in the cavity which was a slot around the circumference of the burner. A theory was developed which adequately predicts the magnitude of the losses for the configuration employed [10]. Figure 12 shows the effect of the damping produced

over a range of equivalence ratios and shows that the damping losses were indeed linear. The slot-groove damper shows great promise as the basis for a hold-off technique. It may also be incorporated as a tunable damper in rocket motors to alleviate acoustic instability with only a slight weight penalty.

A damping device, comprising a 1/2-inch diameter rod inserted opposite the nozzle, was evaluated for possible use as a hold-off technique in standard T-burner practice. It was found to be unsatisfactory because the magnitude of the damping it contributed was insufficient. In the case of small insertion lengths the rod appeared to increase the instability.

VI. PROPELLANT RESPONSE TO THERMAL RADIATION

The complexity of the processes by which a burning solid propellant amplifies pressure waves has defied complete analytical description or adequate experimental characterization. The efforts continue; but, at the present time, it appears that significant contributions to knowledge are unlikely to be developed from the now conventional test devices such as T-burners and L*-burners. New experimental approaches are required, and the recognition of this need to study combustion instability by use of new techniques which would generate more detailed mechanistic information than the usual phenomenological tests motivated the work described here.

All combustion models assume that perturbations in the pressure alter the feedback heat flux to the burning surface and, by this mechanism (as moderated by the coupled thermal wave in the solid), perturb the mass

burning rate. This consideration suggests that another response function, relating mass flux to feedback energy, could be studied with some expectation of defining more precisely the nature of a valid combustion model. In this study, periodic and steady-state radiant-heat fluxes were imposed on the surface of burning strands of propellant, and the changes in regression rates were inferred from measurement of the force resulting from combustion-generated momentum. It was the intent of the work reported here to focus experiment on this coupling function, closely related to the mass-flux/pressure-response function, and, thus, in some degree to investigate the legitimacy of such response functions and to define their nature. Additional information concerning this work is given in a technical report [13] and in two papers [14,15].

A direct measurement was made of the dynamic response of burning solid-propellant strands to an externally imposed, radiant heat flux. Burning-rate changes were determined for both steady and periodic energy fluxes at atmospheric pressure. The strands were mounted at the secondary focus of an elliptical-mirror system, and flux levels to $15 \text{ cal}/(\text{sec})(\text{cm}^2)$ were obtained by use of a 5-kw Xenon-mercury lamp. Steady-state burning rates were obtained by a photographic technique. The periodic variations in mass evolution rates were detected by measurement of the recoil force on the strands. Figure 12 shows the overall experimental system. A quartz-crystal microphone was used as a micro-force transducer.

It was possible to measure the variations in mass efflux from the burning propellant strand produced by the radiant-heat flux. The phase angle between the perturbing flux and the burning-rate response and the dependence of the magnitude of the response on the driving frequency were obtained. Figure 13 shows the measured response at atmospheric pressure

for two AP-polyurethane composite propellants as a function of dimensionless frequency. The real frequency range was from 5 to 150 Hz. The significant effect of propellant transmissivity to thermal radiation which is predicted by theory, is illustrated here. These data can be transformed to yield the real part of the flux-driven response function.

The relationship of the flux-driven response to the pressure-driven case was theoretically demonstrated by solution of the perturbed equations that describe the transient mass and energy flow in the solid and gas phase. The sharp-flame-front model for the gas phase and the same combustion parameters were employed in each case. The pressure-driven response functions were obtained by now conventional manipulations, and the response of the hypothetical opaque propellant to radiant heat flux was obtained in essentially the same manner. In order to obtain the response of the semi-transparent propellant, it was necessary to take advantage of the linearity of the heat-conduction equation and to separately derive the conductive and radiative contribution to the response. These calculations indicate that the flux-driven response, which was measured in this program, is closely related and essentially equivalent to the pressure-driven response at low driving frequencies. Figure 14 shows this comparison.

~~For frequencies somewhat higher than that which produces the maximum in~~
the response function, the calculated flux-driven response decreases rapidly in magnitude, in agreement with the experiment, while the results of the calculated pressure-driven case suggest that some response should be observed even at very high frequencies. The calculations for the semi-transparent propellant show that energy absorption in depth will have little effect at low frequencies but will severely limit the response to radiant fluxes at high frequencies (Figure 14). This strong effect of

transparency is shown experimentally in Figure 13, UAX being more transparent than UCX. A comparison is presented in Figure 15 between the predictions of the flux-driven combustion model (by selection of parameters to fit the UCX data) and the data from the polyurethane-fueled propellants. The PBAA-based UCV and UCW propellant results are also shown for comparison.

The parameters selected to approximate the UCX data are possibly not a unique set, and these results are presented only to illustrate that some agreement between experiment and theory is obtained.

If the combustion model is correct and the data properly interpreted, it should be possible to predict satisfactorily the pressure-driven response or the response under other conditions. A partial test of this approach is illustrated by comparison of the results obtained from the chemically similar opaque UCX and translucent UAX propellants. In the case of the UAX propellant, the same combustion parameters were used in the calculations; but the opacity was reduced to $100/\text{cm}^{-1}$. Although the height of the maximum response function was approximately predicted, the shift in the maximum to a lower frequency was not predicted; and no variation in the model parameters produces a significant change in the position of the response maximum when only the transmissivity was changed. Perhaps condensed-phase energy effects, which were not considered in the calculations, are important for the semitransparent propellant.

Figure 15 also illustrates the observation that propellant formulation changes produce significant variations in the response of the burning propellant to the heat-flux perturbations. The reproducibility and precision of measurement were great enough to permit observation of differences in response for small changes in composition. The overall

characteristics of the response were altered drastically by large compositional variations, such as by change of fuel binder (Figure 15).

The technique for measuring the response function by periodic input of energy to the burning surface holds great promise as a method for characterizing the stability characteristics of a propellant. Not only are the results reproducible for a given propellant, but minor formulation variations produce measurable changes in the measured response functions. This technique has a great advantage over older test-burner methods for measuring response because the driving frequency can be varied over a wide range. Conventional T-burner measurements yield response functions at dimensionless frequencies greater than about 20 (near the maximum response), and the L*-burner tests yield results for dimensionless frequencies in a narrow range of about 5 to 10. When thermal radiation is used as the perturbation source, measurements can be made easily only at atmospheric pressure with opaque, clean-burning propellants; and work to relieve these restrictions while preserving the major advantages of the direct-response measurement technique has been under way and is described in the next section.

VII. PROPELLANT RESPONSE TO ELECTRICAL DISSIPATION AT THE SURFACE

The measurement of the transient burning rate response of propellant strands to radiant energy, described in Section VI, has yielded new insight into the processes responsible for the combustion instability of composite propellants. Unfortunately, this technique can only be applied to fairly opaque, clean-burning propellants. The addition of aluminum to the formulation results in total absorption of the incident radiation, and perturbation of the burning rate by use of external radiation is not

possible. Also, a feasible method for conducting the radiation-perturbed-burning-rate test under pressure is required.

An alternative scheme for introducing the perturbing energy at the propellant surface has been considered in this study. It has been observed [16] that the electrical resistance of AP-composite propellants decreases exponentially with temperature increase, and extrapolation of these data to typical burning surface temperatures shows that the conductivity of a burning strand is low enough to permit introduction of electrical energy. Because of the strong dependence of the strand resistance on temperature and the exponential temperature gradient at the burning surface, for practical purposes the dissipation of electrical energy would occur at the propellant surface. Thus an energy perturbation can be introduced at the surface independent of propellant or flame opacity, and production of adequate electrical input over a wide range of frequencies should be easily realized.

Figure 16 shows the experimental system employed in the preliminary tests. The technique of employing a quartz crystal microphone to measure transient burning rates was borrowed from the studies on radiation-induced burning rate perturbation. The strands were 1 cm. thick by 2 cm. wide and 3 cm. in the direction of burning. Electrical contacts formed of gold foil, tin foil or a silver conductive paint were bonded to the 2 cm. X 3 cm. faces. The thin contact materials were chosen to insure their disappearance with the receding burning surface to minimize electrical conduction through the gas phase.

If the electrical energy dissipation is roughly 5 percent of the energy flux to the propellant surface, it is possible to produce measurable changes in the burning rate. This system was designed to introduce

100 to 150 w at the surface and thus to produce measurable burning rate perturbations at pressures to about 10 atms.

A major experimental and analytical problem is encountered when trying to relate the propellant-response function in which the perturbation energy is introduced at the surface to the response function for pressure variations. In the case of radiant-heat-flux energy as the input, it was possible to relate the two types of response functions through models for the transient combustion process by introduction of the solid transmissivity to the radiation. In the case of the electrical input of energy the same type of approach appears feasible. However, it is necessary to try to account for energy dissipation near the surface in both the gas and the solid phases. A technique was developed and tests were made to determine the path of dc current flow. If this method can be applied to the ac current case, it would yield the information that is required. As an additional check on this accounting a comparison can be made to the existing radiant-heat-flux driven test data on several propellants as a means to evaluate and test the interpretation of the results of ac electrical dissipation.

Figure 17 shows the results of these tests made to determine the path of the electrical conduction. The distinction between the gas-phase and solid-phase path was obtained by burning strands in which mica sheets were cast perpendicular to the burning surface and to the direction of current flow. The flow of current along the solid surface was interrupted as the burning surface reached the mica sheet. Initially, the dc conductivity through the surface was assumed to be due to both solid and gaseous conduction, and as the mica sheet was exposed, the change in conductivity was assumed due to the elimination of electrical current flow along the

solid surface. The results shown in Figure 17 indicate that the electrical dissipation is predominantly in the gas phase at all but the lowest pressures but that a significant fraction of the energy flow is along the surface at the pressures of likely interest in propellant combustion. The analysis of experimental response-function data would be complicated because of the energy release near the surface in both phases.

The really important factor is whether a significant change in burning rate can be produced by electrical current flow along the surface. It was tacitly assumed that a useful analysis could be made if the phenomena can be experimentally shown to produce the desired results.

Figure 18 shows the results of a test in which the burning rate of a strand was determined by continuously weighing on a force transducer. A significant, rapid change in burning rate was produced by introduction of an electrical current flow across the surface. The tendency of the current flow to produce "coning" of the sample indicated a potential problem in analysis of such data. Nevertheless, the results of such tests encouraged evaluation of this technique for ac currents by use of the system shown in Figure 16.

Tests were made only with 60 Hz power because of the convenience of such a source and because it was possible to evaluate the technique without assembly of complicated oscillators and power amplifiers. Only semi-qualitative data were obtained. Significant recoil forces were measured when the electrical current was introduced. The magnitude of the signal and the signal-to-noise ratio was about the same as encountered in the periodic-heat-flux tests with the same arrangement. The preliminary indications were encouraging. However, a more detailed spectral analysis

of the transducer signal indicates a predominance of a 60 Hz signal rather than the expected 120 Hz force signal which should result from the equal dissipation of positive and negative segments of the cycle. This 60 Hz signal was not a result of capacitive coupling since it was not present in the absence of the flame. Apparently, some type of combustion-related process is responsible. Thus, it appears that not only is the electrical dissipation process complicated by the existence of two paths for the current flow, but peculiarities of the electrical dissipation in the combustion zone also produce spurious, unexplained signals. As a result of these complications, efforts to apply the electrical perturbation technique have been abandoned. However, it is likely that a determined, persistent effort to develop this approach would yield a very useful method for characterizing the transient processes of propellant combustion.

VIII. PROPELLANT FLAME TEMPERATURES DURING DEPRESSURIZATION

In previously reported work [17] composite-propellant flame temperatures were measured during depressurization to aid in the interpretations of infrared-emission spectra. Very large transient decreases in these flame temperatures were noted during rapid pressure decay. Although some compositional changes were observed also, and these could account for a small fraction of the temperature drop, order of magnitude calculations showed that they could not be the major cause. It is surmised that the temperature excursions were associated with the requirement to increase the energy in the solid phase thermal wave during a period of decreasing burning rate. The work described here was undertaken with the expectation that transient flame temperature measurements could be used to estimate

the effective variations in propellant burning rate during rapid depressurization. Reference [18] presents the detailed results of this experiment and a paper [19] has been present which was derived from these results.

Figure 19 shows the test chamber, which was attached to the 200 cm. long rarefaction tube of 5.25 cm. diameter. This tube discharged into a 120 liter evacuated tank. Temperatures were measured by the emission and absorption of the sodium D-lines by passing radiation through windows. In order to produce sodium emission, saturated NaCl solution was injected along the axis of the sample. The optical system focus was 0.5 to 1.0 cm. in front of the strand during measurements.

At the beginning of a test, the discharge end of the rarefaction tube was terminated by a cellulose-acetate diaphragm. After ignition and a predetermined burning time of the strands, a run was started when the diaphragm was ruptured with a solenoid-driven needle. An orifice mounted between the diaphragm and the rarefaction tube controlled the rate of pressure drop.

Transient flame temperature measurements were made during pressure decay for two PBAA- and two polyurethane-fueled propellants. Figure 20 shows typical results. The decrease in temperature from the adiabatic flame temperature during pressure decrease was assumed to be related to the change in ratio of the subsurface heat flux to the instantaneous burning rate. It is possible to obtain transient burning rates from such measurements, if one assumes a reasonable time-dependent functional relationship between the flux and burning rate [18]. When such a strategy is employed, it is found that the apparent regression rate remains

constant for 0.5 to 1.0 msec after start of the rapid pressure decay and then quickly decreases to values below the steady-state burning rate corresponding to the instantaneous pressure. The dashed line in Figure 20 labeled r_f/r_0 (the ratio of final to steady-state burning rates for the observed pressure) represents flame temperatures calculated by use of the relationship requiring the assumptions cited above. Only qualitative agreement between calculation and experiment is noted.

Flame temperature measurements with catalyzed and uncatalyzed PBAA and polyurethane fuel propellants produced the curious results that for a given AP-binder system, the high-pressure-flame-temperature histories during depressurization were the same for catalyzed and uncatalyzed propellants. The addition of the burning rate catalyst produced a two or three-fold increasing in the burning rate, and it would be expected that the faster burning propellants would be more insensitive to a given pressure decay rate and would show a smaller drop in the flame temperature than the uncatalyzed systems. It was noted however, that for the system studied, the minimum pressure to produce total extinguishment was significantly reduced by addition of the catalyst.

Consideration of the absence of effect of burning rate on the transient flame temperatures led to a different analysis and interpretation of these data. In this analysis, transient burning rates were estimated from the flame-temperature data by inclusion of the convective terms in the energy balance between the burning surface and the plane of temperature measurement. The changes of feedback flux from the gas phase to the solid surface are assumed negligible. When the data are interpreted in this manner, the calculated transient burning rate appears to drop to a very

low value soon after start of the pressure decay and to remain low until recovery or extinguishment occurs. The gas in the focus of the optical system simply undergoes an isentropic expansion. The dashed line labeled $\Delta S = 0$ in Figure 20 represents calculations based upon these assumptions and the agreement between observation and calculation is remarkable.

A second objective of this work was to investigate further an observation of Schulz [17] that the final system pressure is a critical factor in determining flame extinguishment even when the terminal pressure is much greater than the low-pressure deflagration limit of the propellant. In the present study, tests were made at each of several initial pressures with the terminal system pressure being progressively lowered from test to test until extinguishment by depressurization was obtained. The effective final pressure for extinguishment was obtained as a function of both the initial pressure and the depressurization rate.

Table 1.

Summary of Extinction Data

| Sample | Orifice Diameter inch | Initial Pressure psia | Limiting Pressures psia | | Photo-cell Zero psia |
|--------|--------------------------|--------------------------|----------------------------|-----------------|----------------------------|
| | | | Initial Dump-tank | Final System | |
| UAM* | 0.5 | 92.4 | 7.1 | 11.2 | 14.5 |
| UAM | 0.5 | 192.4 | 3.4 | 11.7 | 23.3 |
| UAT | 1.0 | 82.4 | 8.4 | 12.0 | 23.6 |
| UAT | 1.0 | 182.4 | 7.9 | 15.0 | 32.7 |
| UAB | 1.5 | 92.4 | 4.9 | 9.0 | 17.8 |
| UAB | 1.5 | 182.4 | 3.4 | 10.9 | 36.1 |

* The propellant compositions are UAM (82% AP, 18% PU), UAT (80% AP, 18% PU, 2% catalyst), and UAB (85% AP, 15% PBAA).

Table I summarizes the extinguishment results for the several propellants studied. In these tests, the initial dump-tank pressure was decreased on successive runs until an extinction pressure limit was obtained. The orifice sizes which terminated the rarefaction tube were selected for each propellant to give a near-atmospheric final system pressure at the extinguishment limit. Although the initial time-temperature histories for the catalyzed and uncatalyzed propellants were the same, lower dump-tank pressures were required to extinguish the catalyzed propellants; and thus to obtain nearly the same terminal pressures, larger orifices were used for the faster burning propellant.

The results in Table I show that to a good approximation, the final system pressure for extinguishment did not depend on the pressure from which depressurization started. Thus, it appears that extinction was really determined by the low pressure processes. The initially higher burning rates and rates of pressure drop at high initial pressures did not have a strong effect on the extinguishment.

Depressurization rates for the tests indicated in Table I were in excess of 100 sec^{-1} . At rates less than 5.0 sec^{-1} , the independence of the final extinguishment pressure of the initial pressure can be more clearly demonstrated, and such results are shown in Figure 21. The phenomena of the early disappearance of the flame without permanent extinguishment unless the pressure drops below a critical value of pressure is clearly illustrated here. This critical extinguishment pressure is a function of the depressurization ratio. This type of results is a major motivation for the work done on the low-pressure-deflagration limit of propellants discussed in the next section.

IX. PROPELLANT EXTINGUISHMENT AND BURNING AT LOW PRESSURES

The phenomena which occur as a composite propellant is extinguished by slow pressure decay at low pressures have never been properly characterized nor adequately explained, and the present study was undertaken to improve our understanding of these important processes. Since the characteristic time and distance scales of these processes are larger than those associated with normal propellant combustion, it is possible to make measurements which would not be practical at higher pressures. Presumably, some of these observations of burning at low-pressure will be applicable to all conditions. Those processes which are characteristic of only low pressures are of interest because they are apparently of prime importance in depressurization extinguishment and in the determination of the low-pressure-deflagration limit of the propellant.

Several catalyzed and uncatalyzed propellant formulations based on the polyurethane, PBAA, HTPB, fluorocarbon and the poly-lauryl-methacrylate binder systems have been used. A few aluminized propellants have been tested. Tests have been conducted from atmospheric pressures down to 0.02 atms. This study has included an evaluation of the effects on the combustion process of oxidizer loading and particle size, pressure and rate of pressure decay, strand size, and temperature. The effects of an external radiation flux imposed on the strand surface and of the chemical nature of the environment gas surrounding the strand were also evaluated. The following paragraphs briefly summarize the observations and preliminary conclusions of this work.

The special test chamber sketched as Figure 22 was designed and built

for this work. Controlled rates of pressure decay were achieved by venting gas from the test chamber into a large vacuum tank, and precision pressure transducers were used to monitor the pressure history. The sample strands were held inside the small furnace which was constructed of resistance-alloy ribbon and a light-weight radiation shield. This furnace could be brought to temperature in 10 to 20 seconds. It was possible to ignite the strands in a cold environment produced by the flow of a temperature-controlled gas past the sample, then rapidly bring the furnace to a desired temperature. The strands thus burned in a controlled thermal environment.

The steady-state and transient burning rates were determined from a record of strand weight as sensed by a sensitive force transducer. Figure 23 shows typical weight-time records for burning of a strand. One advantage of the continuous weight measurement technique is the ease of detection and measurement of irregular burning phenomena. When transient burning rates were to be measured it was necessary to use a jet-deflecting disc mounted above the sample to compensate for the combustion recoil force.

One of the first objectives of this research was to establish low-pressure-deflagration limits, P_{DL} , for the propellant systems of interest. The conventional technique for determining the low-pressure limit by extinguishing strands at lower and lower rates of pressure decay to find an asymptotic limiting pressure was applied to several propellants. It was found that, with some, a minimum extinguishment pressure could not be attained at reasonable rates. In some cases, reproducible data were difficult to obtain. Apparently burning was very sensitive to small perturbations in pressure or flow. Reproducible values of P_{DL} for all systems required nearly disturbance-free conditions. A go/no-go test at

fixed pressure was devised.

Tests were made at a constant pressure close to the pressure-deflagration limit. Strands were ignited with a hot-wire coil which was placed on or near to the sample surface. Transient burning could always be achieved by slow heating of the surface because a thick thermal wave was produced in the solid. If the strand continued to burn after the preheated material in the thick thermal wave was consumed, the pressure was assumed to be equal to or above the deflagration limit; but if the strand extinguished, the pressure was presumably less than P_{DL} . By variation of the chamber pressure, it was thus possible to obtain an accurate measure of the true lower limit of pressure for strand deflagration. Surprisingly, in many cases, these values of P_{DL} were significantly greater than the extinguishment pressures, P_E , measured at very low pressure-drop rates.

The effect of oxidizer size on the deflagration limit was studied for the PBAA and polyurethane propellants systems, and an explanation was obtained of the observation that finer particle size produces higher values of P_{DL} . Figure 24 shows the effect for a polyurethane propellant. An evaluation of this type of data showed that the ratio of the depth of the polymer melt zone to the particle diameter is the critical factor. The polymer melt apparently coats the finer AP particles and inhibits their ignition and burning. The polyurethane system which burns with a relatively thick melted region is unusually strongly affected by decrease of AP size. As shown in Figure 24, the data for the PBAA-fueled propellant, which has a very thin melt zone if it melts at all, indicate values of P_{DL} which are nearly unaffected by particle size variations.

Similar information is given on Figure 25, where the deflagration limit is plotted against AP loading, the AP being, for these propellants,

the bimodal mixture customarily used for high loadings. The reaction-inhibiting effect of molten PU polymer is again apparent. Above a loading of 80%, however, there is not enough melt to produce the effect; the deflagration limit is independent of AP loading. Propellant fueled with poly-lauryl-methacrylate (LMA) behaves similarly. The deflagration limit for a fluorocarbon-fueled propellant (FC), supplied by the Thiokol Chemical Corporation, is found to be above 5 atm.

The propellants containing PBAA as fuel-binder behave strangely. One would expect that the more highly oxidized propellants would have a higher flame temperature and a greater burning rate and would therefore, exhibit lower deflagration limits. In fact, the highest deflagration limits are found for the "hottest" propellants, and the very fuel-rich PBAA propellants (up to 30% polymer) could not be extinguished in the experimental system used. The explanation offered is based on the observation that a significant amount of unburned AP is ejected from the regressing surface when these propellants burn at low pressures, noticeably more at higher AP loadings. It is possible that, for the portion of the propellant that actually burns, the AP/PBAA ratio is higher in the case of the nominally 75% propellant than in that of the nominally 85% propellant. Supporting evidence is that, near the deflagration limit at the same pressure, the 75% propellant has a higher burning rate than the 85% propellant.

At subatmospheric pressures, the flame temperature over the propellant strands is low enough to permit measurement by SiO₂-coated platinum/platinum-rhodium thermocouples. Figure 26 shows that near P_{OL} the measured temperature drops rapidly as the pressure is lowered, and very near the limit, for all propellants tested, the measured temperatures are less than 1300°K or about half the adiabatic flame temperature computed for

equilibrium products. These measured temperatures require a radiation correction of about 100°K to be indicative of the actual flame temperature. While the absolute accuracy of these temperatures is uncertain, the conclusion seems unescapable that the combustion efficiency is very low near P_{DL} . Whether or not final extinguishment results when the flame temperature drops below some critical value is a subject for conjecture.

The pressure-deflagration limit as defined above is not a property of the propellant alone. It depends also on the temperature of the surroundings with which the propellant reaction zone is in thermal communication. In all the experiments so far reported, the chamber temperature was, initially at least, at the normal room temperature. It was possible, by use of the furnace shown in Figure 22, to investigate the effect on extinguishment pressure of heating the surroundings to compensate for heat losses. After the propellant was ignited, the furnace was quickly brought to a preassigned temperature (measured on the Nichrome); and depressurization started. Prior calibration of the furnace allowed reporting of an effective furnace temperature, the temperature of black-body surroundings giving the same radiant heat flux at the sample position.

Figure 27 shows the results for the fluorocarbon-fueled propellant. At room temperature, the extinguishment pressure is just over 5 atm, as also shown on Figure 25. When, in successive tests, the effective furnace temperature was raised, the extinguishment pressure dropped drastically until, at 700°C, the burning could not be extinguished at the lowest attainable pressures. Data scatter is less pronounced if only the data taken with nitrogen as ambient gas are considered. At effective furnace temperatures below about 420°C, burning was irregular, as indicated by a

fluctuating weight signal. Extinguished surfaces were visibly rough. At higher effective temperatures, extinguished surfaces were smooth; and the weight-time record was also smooth.

The same qualitative results were obtained with propellants containing the hydrocarbon-based fuel polymers, except that the reduction in extinguishment pressure was less pronounced at effective furnace temperatures below 400°C. Figure 28 shows typical results. In no case did the propellants extinguish if the effective temperature was as high as 700°C.

Near the deflagration limit the surface temperatures (measured by embedded thermocouples) are near 300°C, and the flame temperatures are about 1300°C, and it appears that the significant changes in strand values of P_{DL} occur for energy inputs characteristic of temperatures of 500 to 700°C. The elimination of radiant heat loss from the surface by surrounding the strand with the furnace at 300°C does not produce significant changes in P_{DL} . Changes are produced at the somewhat higher temperatures which approach those of the expected surface temperatures at high pressures. Also it appears that these changes in P_{DL} are produced without a significant reduction in the radiant heat loss from the flame, since even at the highest furnace temperatures, the radiation flux from the flame would greatly exceed the heat flux from the furnace.

Once it was established that, at low pressures and low depressurization rates, the extinguishment pressure was independent of initial pressure (see Figure 21 for example), it was possible to prepare a plot such as Figure 29 of the extinguishment pressure versus the depressurization rate without consideration of initial pressure as a parameter. The results shown here are for strands burned in the apparatus depicted in Figure 22

but with the heater removed. Extinguishment was determined in many cases both by constancy of the sample weight and by disappearance of a light signal from the flame. At the lowest depressurization rates, extinguishment occurs at an asymptotic pressure which, for most propellants, is the value of P_{OL} measured by the go/no-go criterion. At higher depressurization rates, extinguishment occurs as a result of the inability of the solid phase to respond to the depressurization. In this case, the characteristic time constant of the thermal wave response, κ/r^2 (where κ is the solid thermal diffusivity and r the steady-state burning rate at the existing pressure) becomes larger than the value of $(d\ln p/dt)^{-1}$ which is the characteristic time of the pressure decay. Although the time scale is different, the phenomena observed are presumably the same as in extinguishment at depressurization rates in excess of 100 sec^{-1} .

Because the low pressure processes are relatively slow phenomena (total test times varied from 10 to 200 seconds) it was possible to measure directly transient burning rates during depressurization by weighing the strands. Figure 30 shows interesting, apparently anomalous results for two similar propellants containing different binders. These four tests were made at the same depressurization rate of 0.075 sec^{-1} . The polyurethane-fueled propellant followed the steady-state burning to low pressure and then abruptly stopped burning. In contrast, the faster burning PBAA propellant showed a deviation from the steady-state burning rate at a relatively high pressure and then a continuous drop in burning rate until extinguishment occurred near the value of P_{OL} . Deviation from the steady-state burning rate would be expected to occur at a higher pressure for the slower-burning propellant. The anomaly can be explained by reference to Figure 29. The test conditions for the PBAA propellant resulted in

extinguishment in the low depressurization range where extinguishment was the result of approach to P_{DL} . In the case of the polyurethane propellant, extinguishment occurred in the higher pressure region where extinguishment apparently occurred because of inability of the propellant to respond to the pressure changes.

If the depressurization rate is increased for the polyurethane propellants, extinguishment occurs at higher pressures and deviation from the steady-state value of the burning rate occurs before extinguishment. Unfortunately it was not possible to follow burning-rate changes by use of the force transducer at depressurization rates in excess of about 1 sec^{-1} because of noise generated by gas flow in the body of the transducer. An attempt was made to characterize the deviation from steady state during rapid pressure decay by measurement of the electrical conductivity across the burning surface. Figure 31 shows the results of several rarefaction tube tests on a polyurethane propellant. If the depressurization rate is less than about 0.1 sec^{-1} , the measured conductivity follows the steady state curve. At high depressurization rates, the conductivity drops to the extinguished value at higher and higher pressures as the rate of pressure drop increases. Presumably this result indicates earlier and earlier deviation from the steady-state conditions at the burning surface. This result is consistent with the suggestion made earlier that at high rates (greater than the 200 sec^{-1} rate observed in the test described by Figure 20), the deviation from equilibrium conditions would occur soon after the start of depressurization and that a near zero burning rate would result.

The low pressure combustion studies discussed in this section have been essentially completed. After some additional tests and further data analysis

and interpretation, a technical report will be issued giving the details of the work. A paper [20] has already been presented outlining some of the results of this study.

SUMMARY

The research reported encompasses studies of several aspects of the combustion of AP-oxidized composite propellants. The results of ignition by electrically heated imbedded wires reveal that there are apparently two sets of ignition reactions, one confined to material at the propellant surface and the other occurring in depth.

In the study of low-frequency, L^* , combustion instability it was found that, by reducing L^* one can induce L^* instability. Thus (1) the stability criterion established by testing with increasing L^* is validated, and (2) it is confirmed that L^* instability is self-excited. A modular theory has been proposed and applied in simplified form.

Acoustic instability was investigated in three ways. A radial-mode analog of the T-burner was developed, the expectation being that problems arising in the interpretation of T-burner data might be solved. Producing oscillations in the first radial mode, unmixed with first and second tangential modes, proved to be very difficult. A comparison of oscillation growth constants--first tangential mode in the radial burner vs. the first longitudinal mode in a T-burner--did not yield the expected relationship, probably because of excessive losses in the radial burner.

In the second study of acoustic instability, a gas-fired (methane, nitrogen, oxygen) T-burner was tested. Despite the fact that the pressure-flow rate phase relationship is opposite to that attributed to the propellant-fired burner, the gas-fired burner amplified self-excited acoustic

oscillations in much the same way. Two instability maxima were observed, one for lean and the other for rich mixtures. There is a strong inference that gas-phase reactions play a role in instability, and a consequent suggestion that the same may be true in the propellant-fired burner and in operational rocket engines.

In the final study of oscillatory burning the burning-rate response, measured by the combustion recoil force, to a periodic external radiant heat flux was measured. The burning rate-pressure response function was inferred, and compared to that predicted by current theories of acoustic instability.

The flame temperature close to the surface of the burning propellant was measured optically while the pressure was dropped rapidly by a rarefaction wave. Previous studies had shown that variations in gas composition resulted from rapid pressure change, but later analysis indicated that they could not account for the magnitude of the temperature excursions also observed. It is now surmised that these excursions were due in large part to energy demands of the solid thermal wave during a period of decreasing burning rate.

An extensive study of combustion at the lowest pressures at which unaugmented combustion can persist showed a strong effect of the properties of the polymer used. Polymers that liquefy readily (polyurethane and poly-lauryl-methacrylate) extinguish at higher pressures than others. On the other hand, at high AP loadings these propellants and others with dissimilar polymer fuels extinguish at nearly the same pressure in a given thermal environment. Two regimes of extinguishment by pressure drop are discerned. At higher rates of depressurization, higher extinguishment pressures are found, as determined in large part by the fact that the

ratio of the characteristic times (depressurization and relaxation of the thermal wave) is reduced. At very low rates of depressurization, the extinguishment pressure becomes independent of the rate, and is in some cases lower than the deflagration limit determined in constant pressure experiments.

The general philosophy of the related projects has been that we expect to gain knowledge of the mechanism of combustion by studying both flames existing under conditions of marginal stability and flames subjected to externally imposed transient conditions. The complex set of coupled phenomena that comprise combustion does not yield easily to analysis, but some generalizations are beginning to appear. One is that, particularly at low pressure, a propellant flame can persist in a metastable state, dying out only after a significant period of time, unless externally perturbed. Another is that oscillatory combustion can occur at frequencies characteristic of the propellant, and without continued excitation by or coupling with pressure or flow disturbances. Still another is that gas-phase chemistry probably plays a much more important role in propellant combustion than is generally believed. Placement of these generalizations on a quantitative foundation is in a primitive but progressing state of development.

APPENDIX A

FIGURES

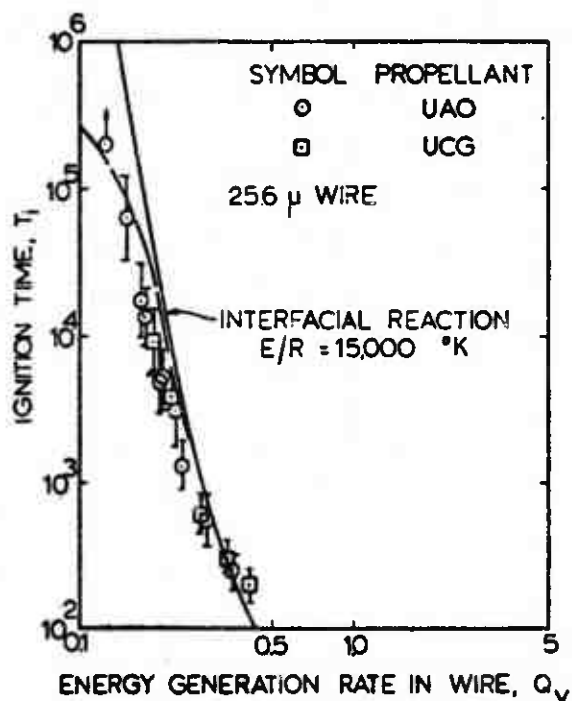


Figure 1. A comparison of computed and experimental ignition times for a 25.6 micron diameter wire. The dashed line extending from the solid line in the upper left corner results from the addition of a distributed reaction ($E_v/R = 5000^\circ\text{K}$) into the interfacial reaction model. Ignition time range 0.1 to 20 seconds. The UCG and UAO propellants contained 80 percent and 72 percent AP respectively in PBAA. Both contained 2 percent Harshaw CU-0202P catalyst.

$$\text{Here } Q_v = \frac{a^2 q_v}{2k v_0}, \quad T = \frac{\kappa t}{a^2}.$$

κ is the propellant thermal diffusivity, t is time, "a" is the wire radius; k is the propellant thermal conductivity; v_0 is the initial solid temperature (300°K in all tests); and q_v is the volumetric rate of energy generation in the wire.

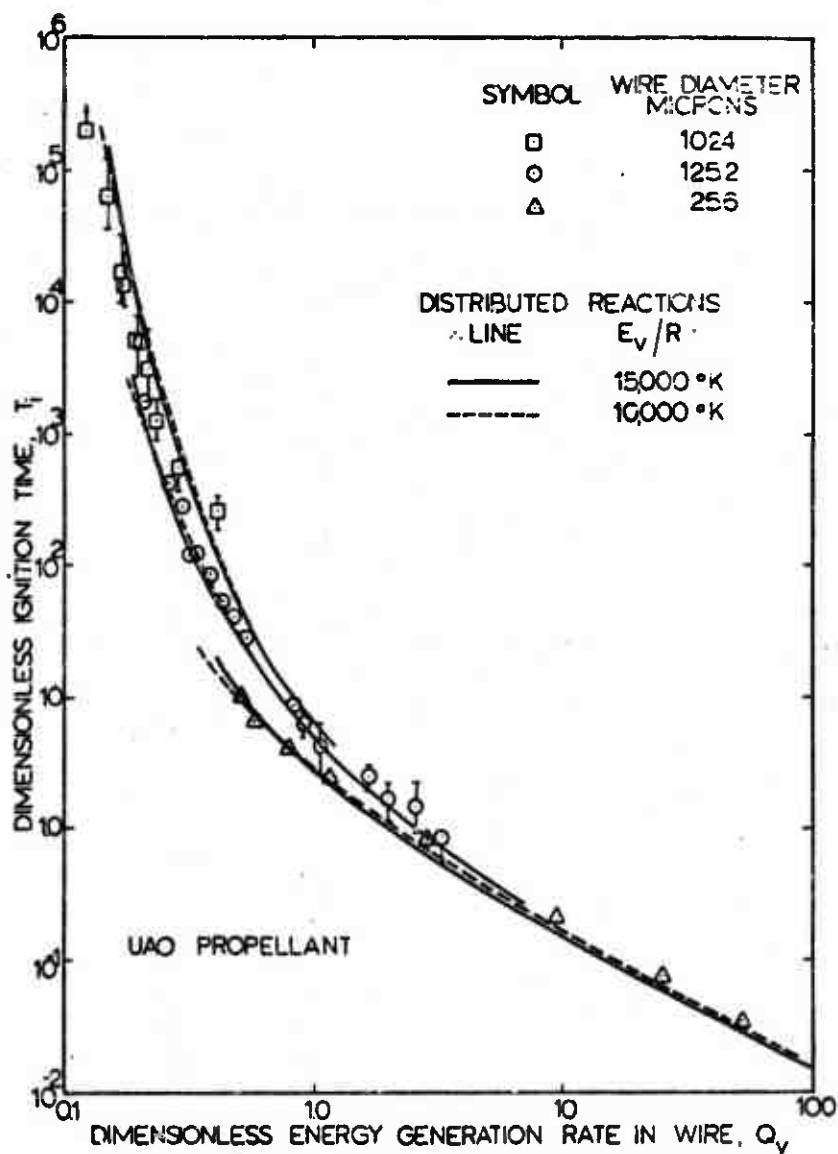


Figure 2. A comparison of experimental ignition times to those from a two-reaction model. The interfacial-reaction parameters are the same as for Figure 1. The activation energies of the distributed reactions are indicated by the lines.

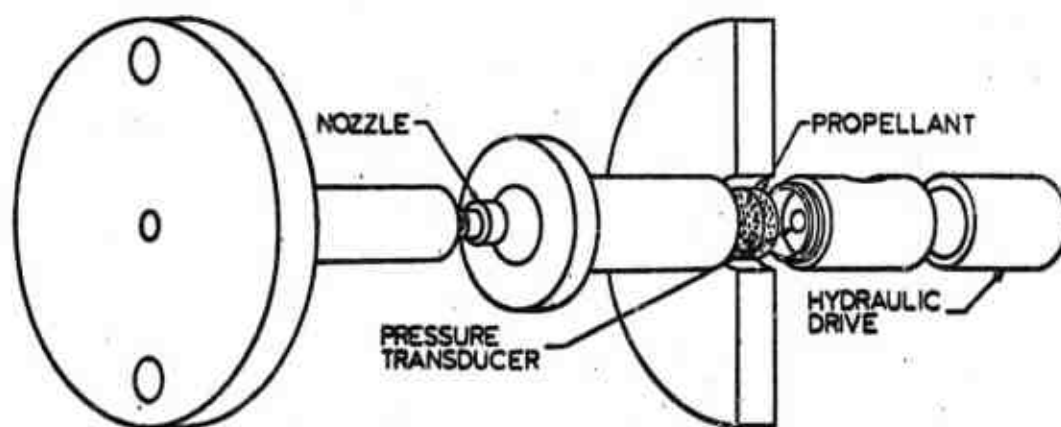


Figure 3. A sketch of the modified L^* burner. The hydraulic drive moved the propellant toward the nozzle to reduce L^* during a test.

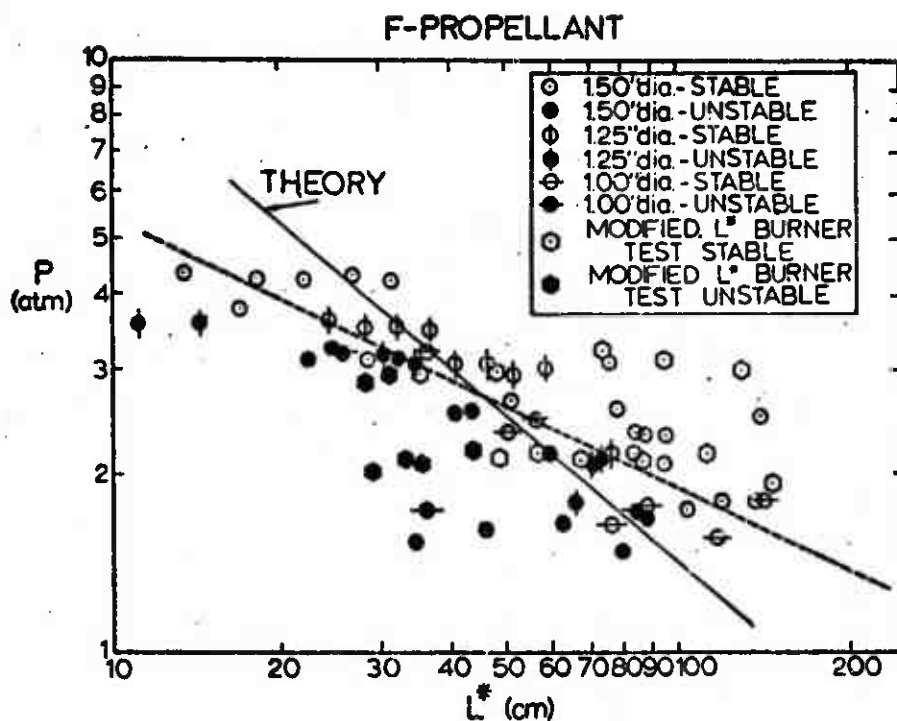


Figure 4. A comparison of the measured and theoretical stability limits in the L^* burner. Shown are data from a conventional burner (L^* increases) and the modified burner (L^* decreases). The F-propellant tested here is 80 percent AP in PBAA with 2 percent Harshaw CU-0202P catalyst.

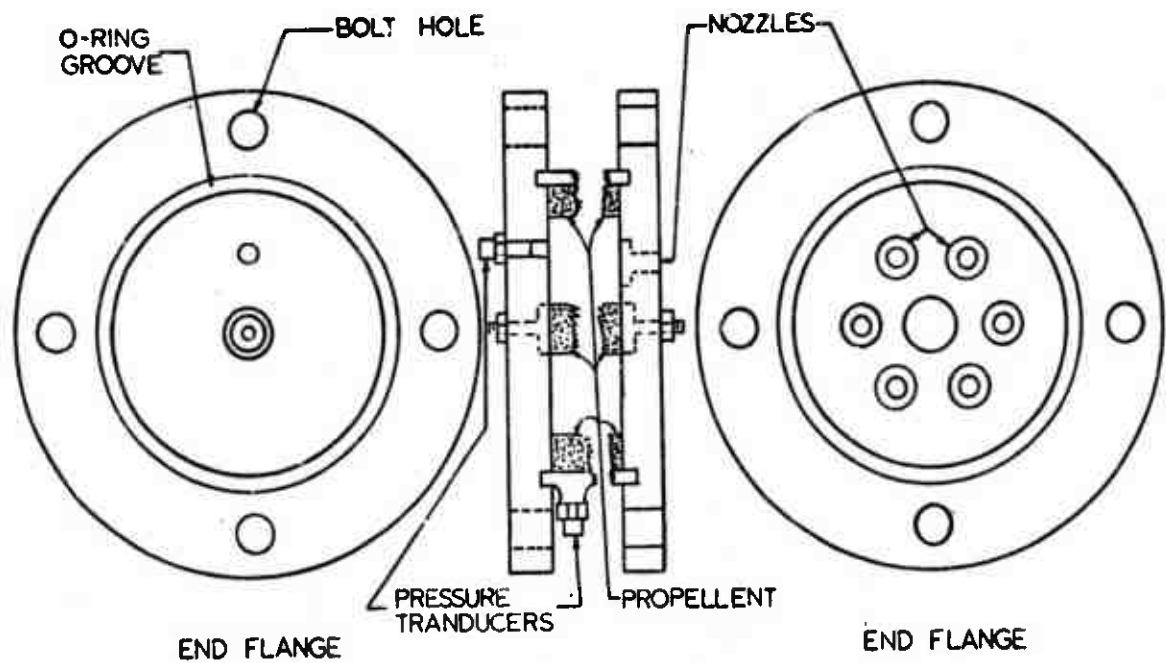


Figure 5. The radial-flow, radial-mode burner is sketched here.

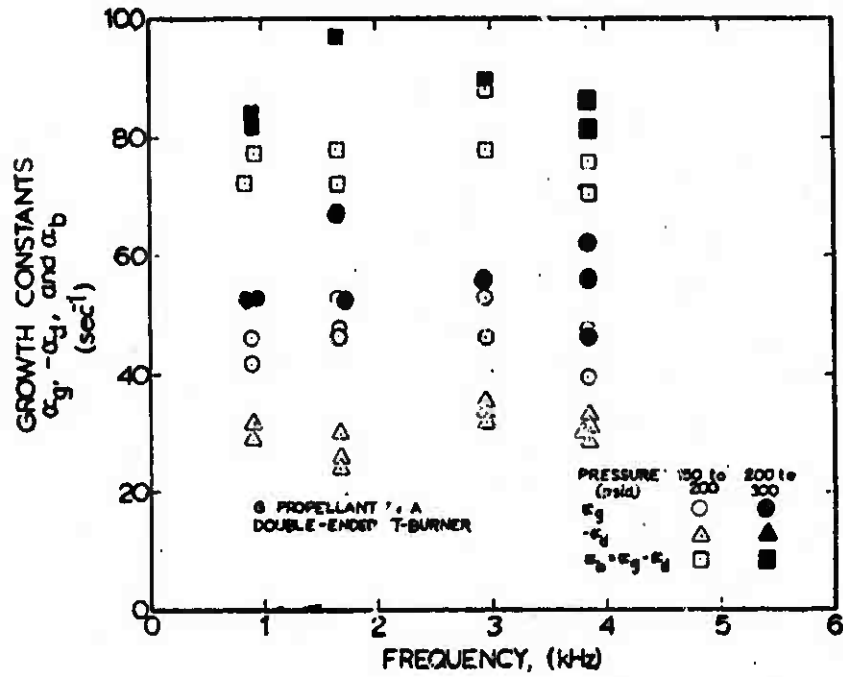


Figure 6. Growth constants measured in a double-ended T-burner for the G propellant are shown here. The G propellant contained 82 percent AP in 18 percent PBAA.

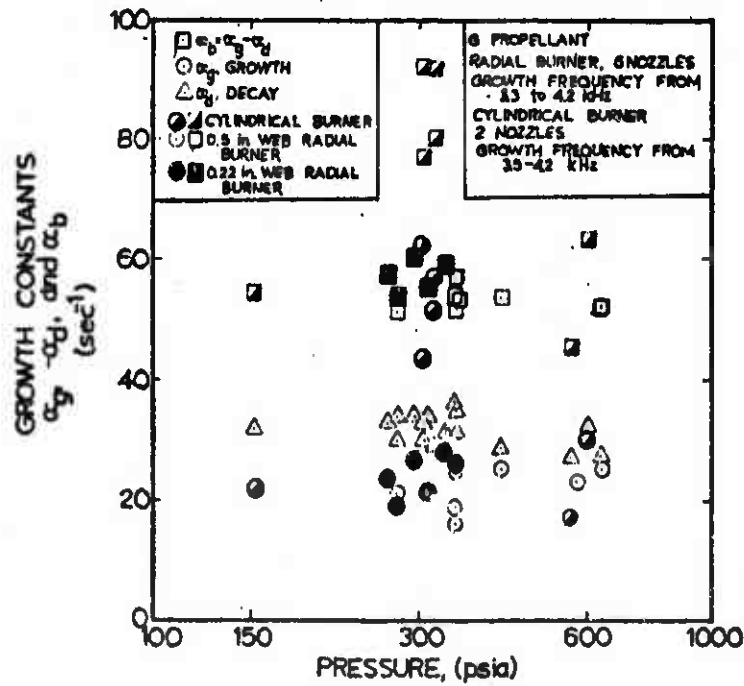


Figure 7. Growth constants measured in the burner shown in Figure 5 for the G propellant are shown.

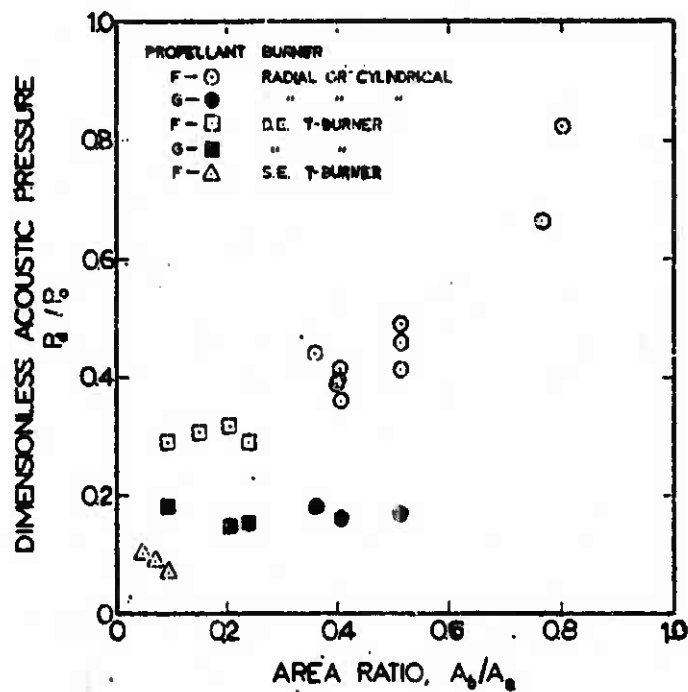


Figure 8. The magnitude of acoustic pressure oscillations as a function of the ratio of energy input (propellant area) to energy losses (inert wall area) is shown here. The data are averaged over a mean chamber pressure from 150 to 600 psia.

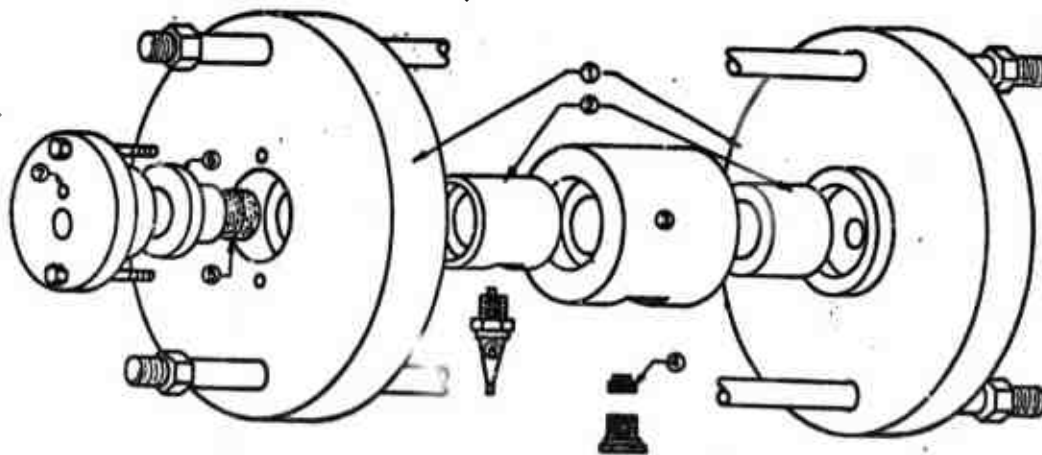


Figure 9. An exploded view of the gas-fueled burner is shown here. The numbers correspond to:

- | | |
|---------------------|-------------------|
| 1. End flanges | 5. Permeable disc |
| 2. Chamber sections | 6. Disc holder |
| 3. Nozzle section | 7. Fuel inlet |
| 4. Graphite nozzle | 8. Spark plug |

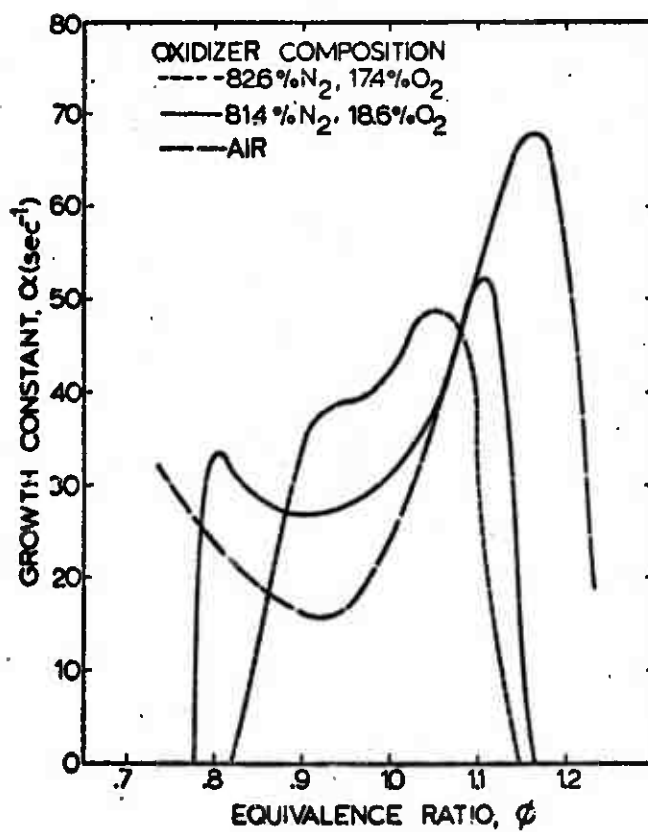


Figure 10. The effect of increased nitrogen dilution on the relationship between the growth constant and equivalence ratio. Except for the oxidizer-stream composition, all runs were made at 100 psig and 10 gm/sec total flow with CH₄ fuel.

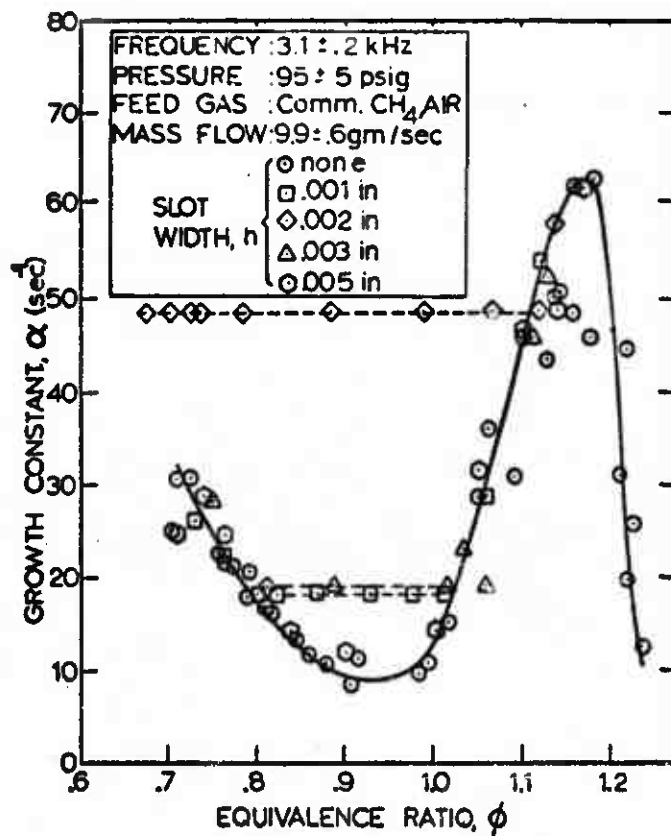


Figure 11. Growth constants for air-CH₄ combustion in the burner shown in Figure 9. The effect of the perimetrical slot width is shown.

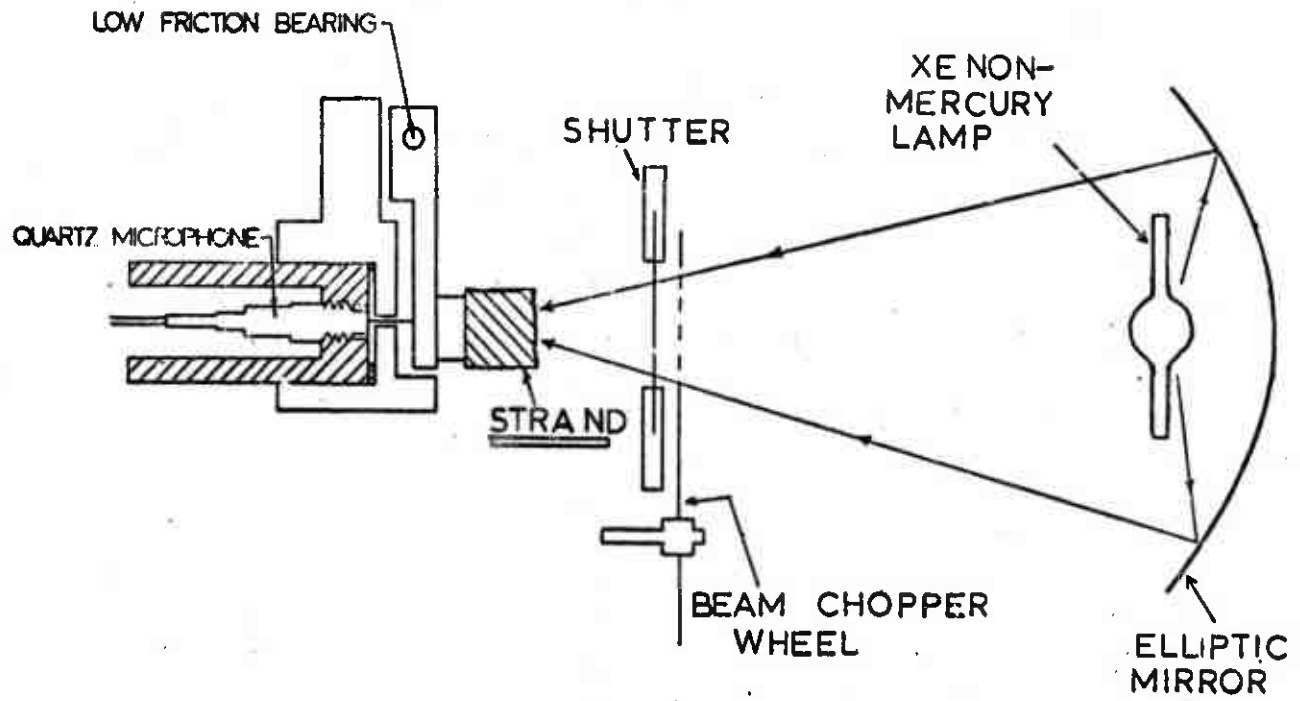


Figure 12. A sketch of the overall experimental system for the combustion-recoil experiment is shown.

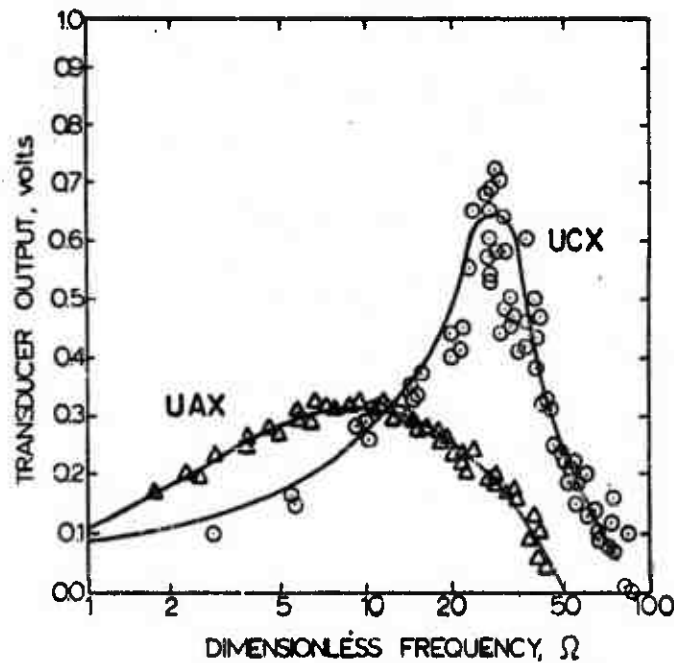


Figure 13. The response of polyurethane fueled propellants to periodic heat flux variation as a function of the dimensionless flux frequency. The dimensionless frequency is $\Omega = \kappa\omega/r^2$ where κ is the thermal diffusivity, ω the actual radian frequency and r the burning rate. The opaque UCX propellant contained 80 percent AP, 17 percent Estane-type polyurethane, 1 percent carbon black and 2 percent n-butyl ferrocene catalyst. In the UAX propellant, the 1 percent carbon black of the UCX formulation was replaced by polymer.

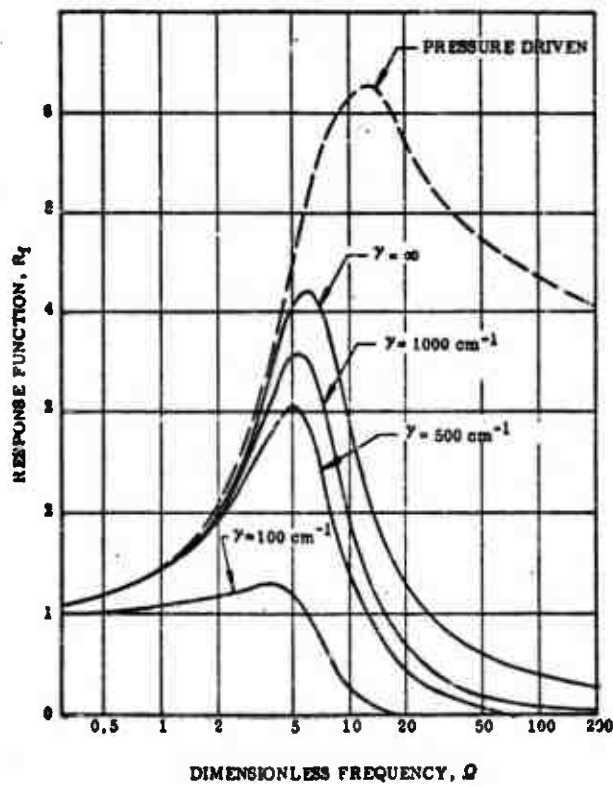


Figure 14. A comparison of the computed real part of the response functions for the pressure and heat flux-driven oscillations of a burning solid propellant. The same parameters were used in each case; γ is the solid opacity.

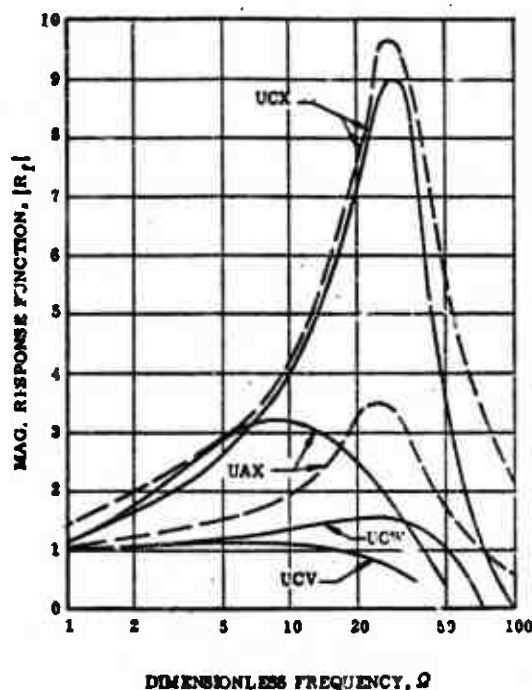


Figure 15. A comparison between the magnitude of the response functions calculated from the modified conventional theory and experimental values. The dash lines are for the calculated values. The UCV and UCN propellants contained 80 percent AP in PBAA. The former contained 2 percent Harshaw CU-0202P; the latter contained 1 percent carbon black.

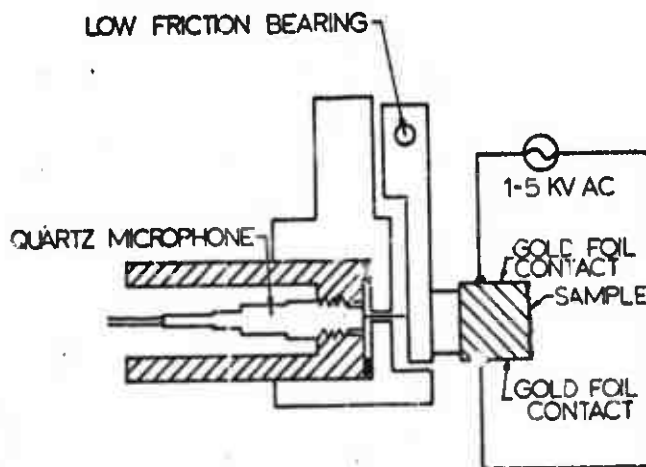


Figure 16. A sketch of the experimental system for measuring combustion recoil with electrical energy input to the burning surface.

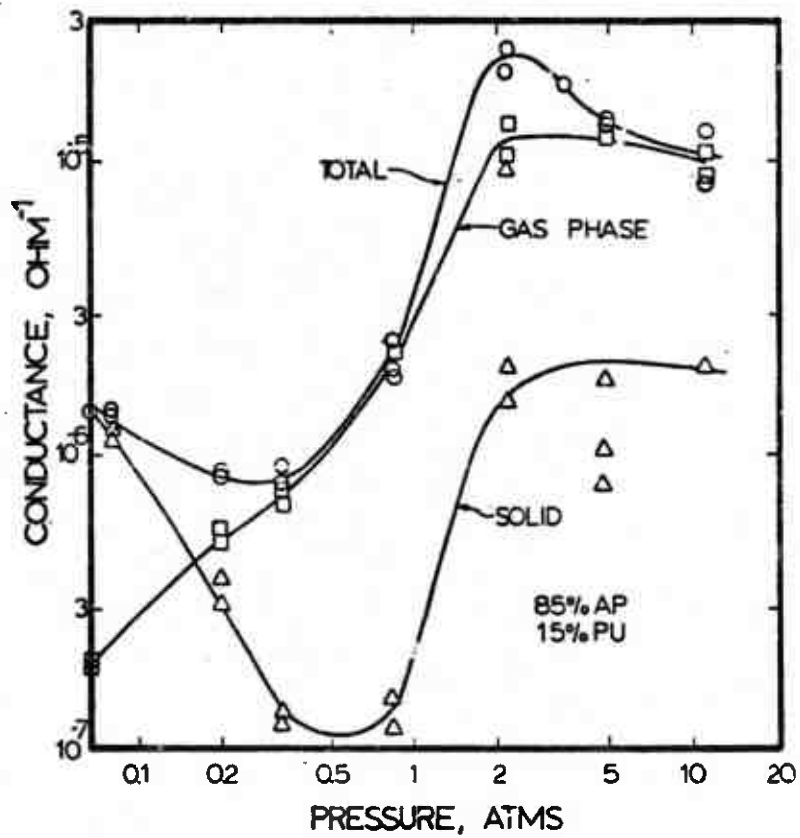


Figure 17. The conductance of burning 1/2 X 1 cm. propellant strands as a function of pressure.

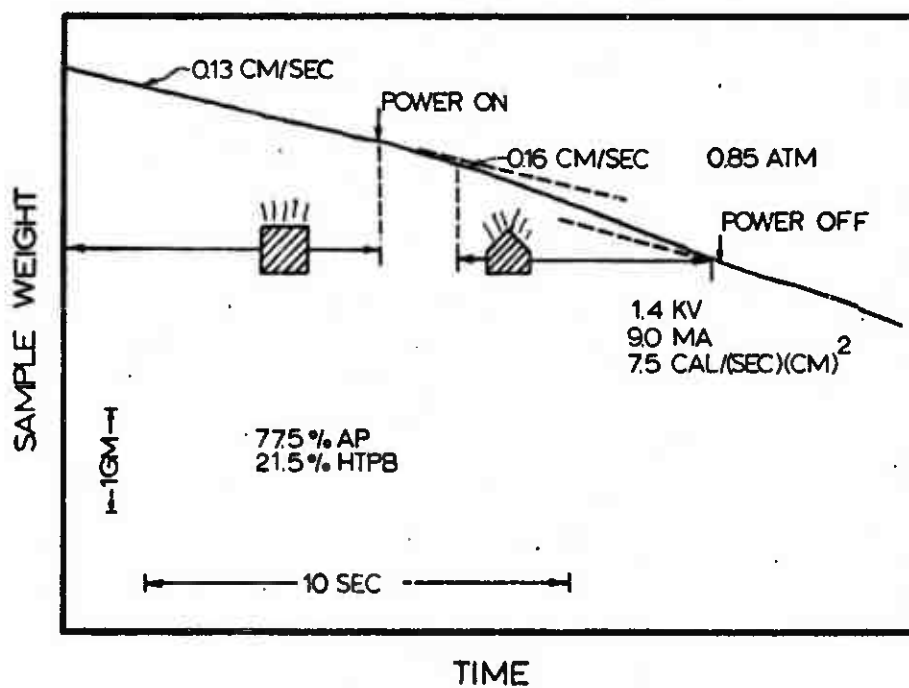


Figure 18. Measured changes in burning rate by input of dc energy at the surface of a burning strand.

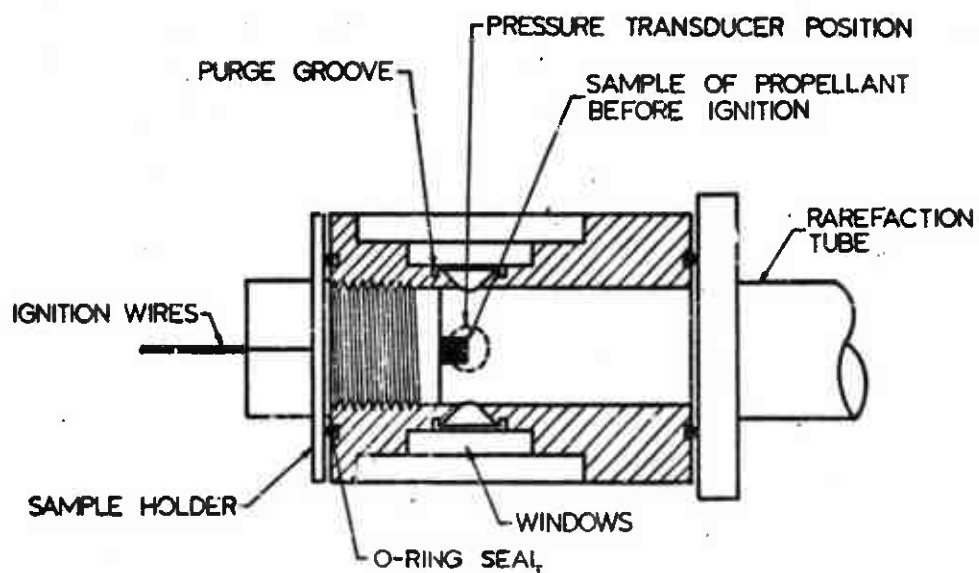


Figure 19. A side section of the test section which was mounted on the rarefaction tube (shown on the right). The surface of the extinguished strands was flush with the end of the test section and 0.5 - 1 cm. from the focal plane of the optical system.

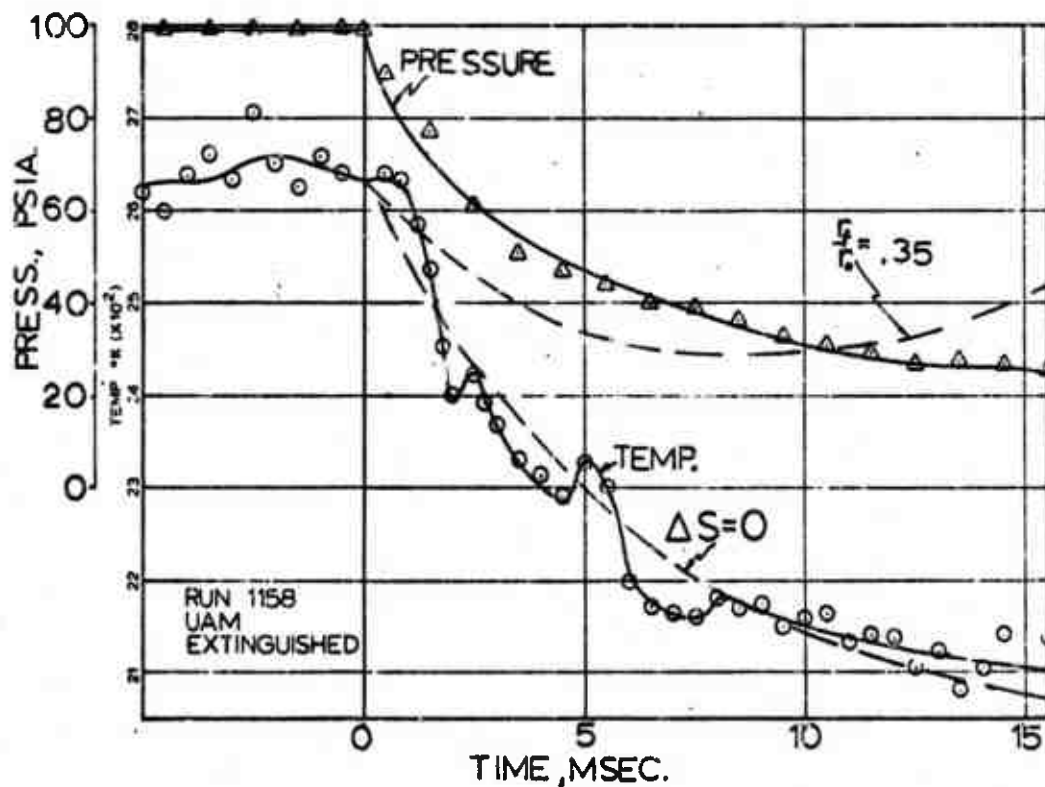


Figure 20. Measured pressure, temperature data for the uncatalyzed UAM polyurethane propellant at a high pressure decay rate. The upper dashed line was drawn from results computed as described in reference [19], and the low dashed line represents a history for simple expansion of the combustion gases. The UAM propellant contained 82 percent AP and 20 percent PU.

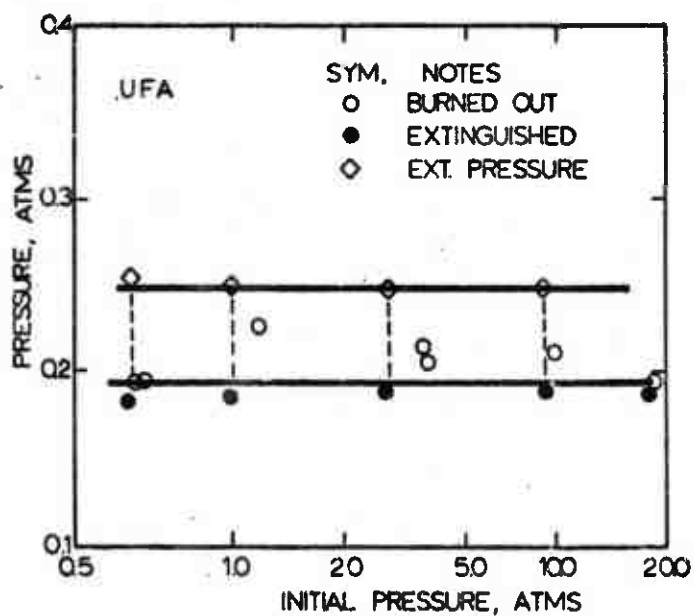


Figure 21. Extinguishment pressures for the 80 percent-AP polyurethane-fueled UFA Propellant. A depressurization rate of 5 sec^{-1} was used. Initial chamber pressures are indicated.

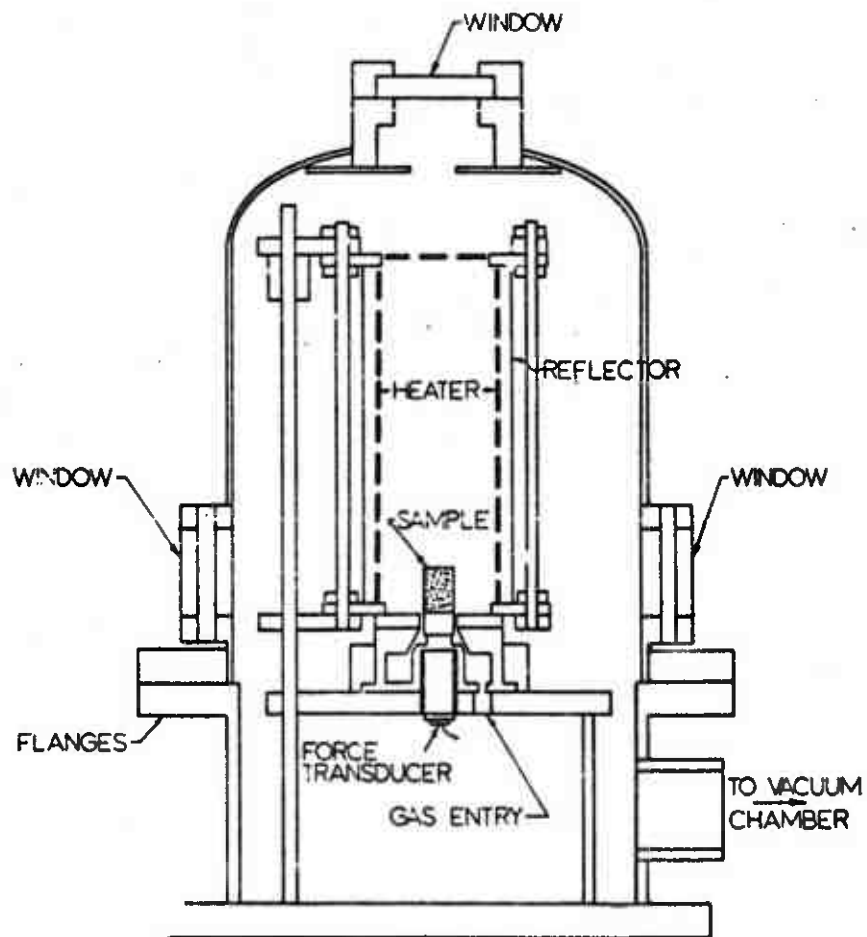


Figure 22. Schematic sketch of the 25-cm-diameter combustion chamber used in these tests. The chamber was vented, through orifices, when appropriate, into a large vacuum tank.

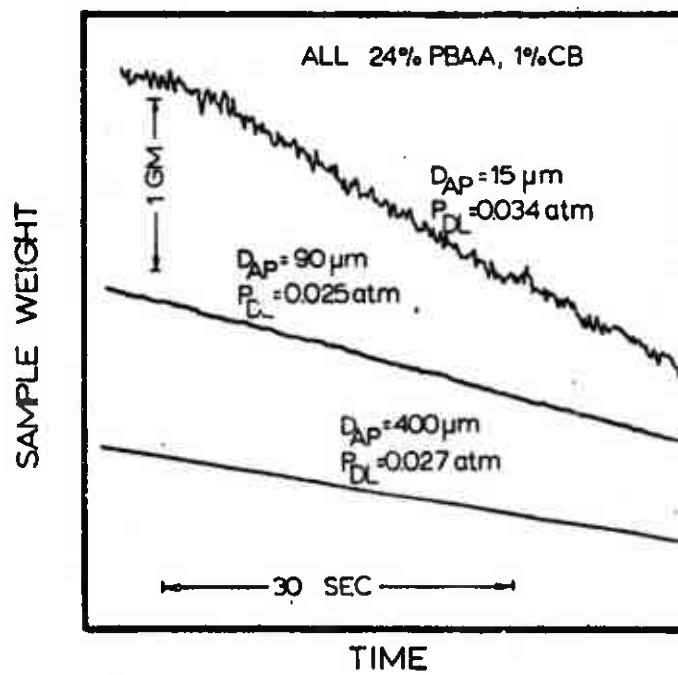


Figure 23. Measure of sample weights near P_{DL} as a function of time for an AP propellant.

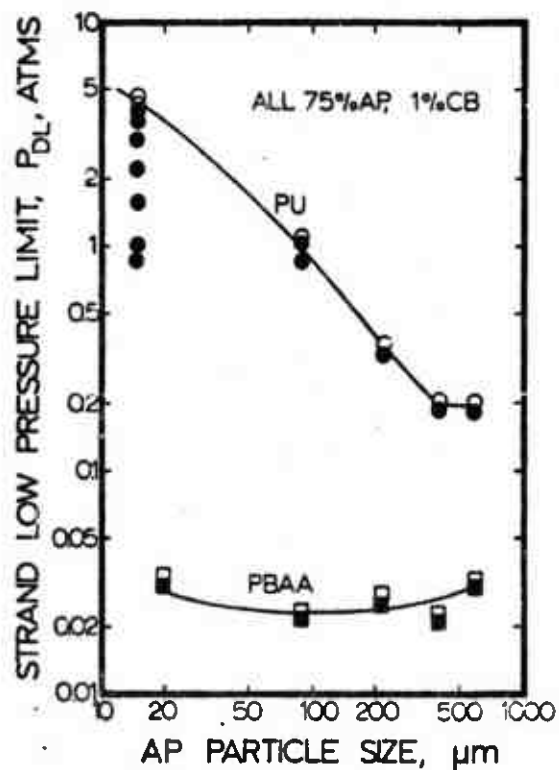


Figure 24. The low-pressure deflagration limit for strands of two series of 75 percent-AP, 1 percent-carbon-black propellants is indicated here. Tests were made by the go/no-go ignition procedure, and a single size of AP was used in each formulation. The open symbols indicate conditions in which strands completely burned, while the filled symbols indicate conditions in which strands were not consumed.

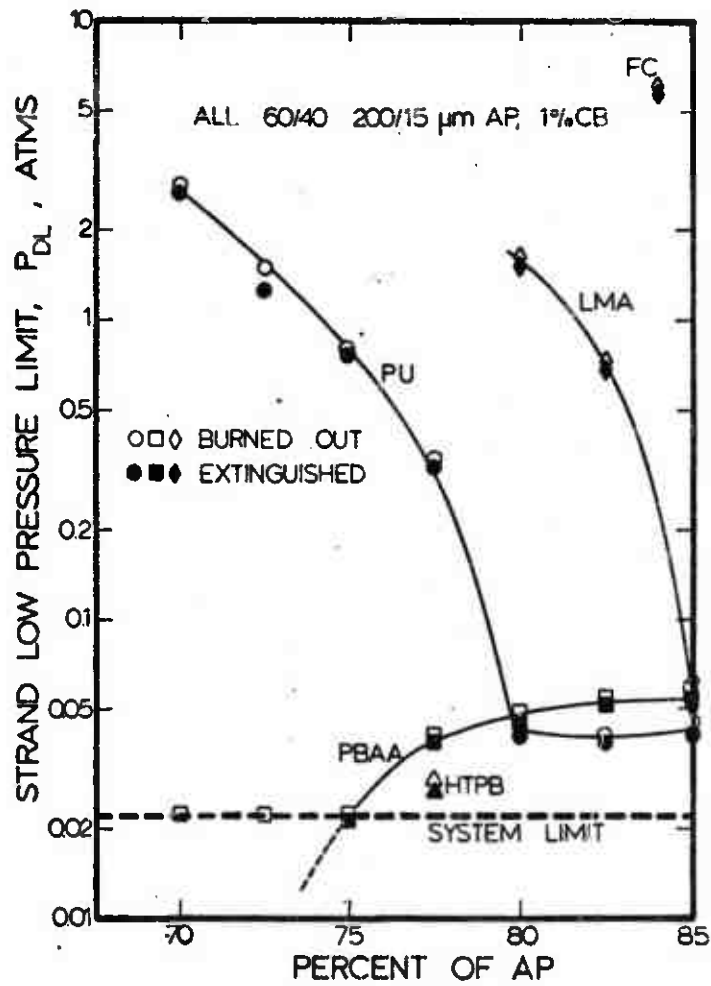


Figure 25. The deflagration limit for a series of bimodal AP propellants is indicated here, as measured by the go/no-go ignition technique. All propellants contained 1 percent carbon black and were uncatalyzed. The interpretation of the open and filled symbols is as for Figure 24. The system-limiting pressure was the minimum attainable pressure in the large vacuum tank.

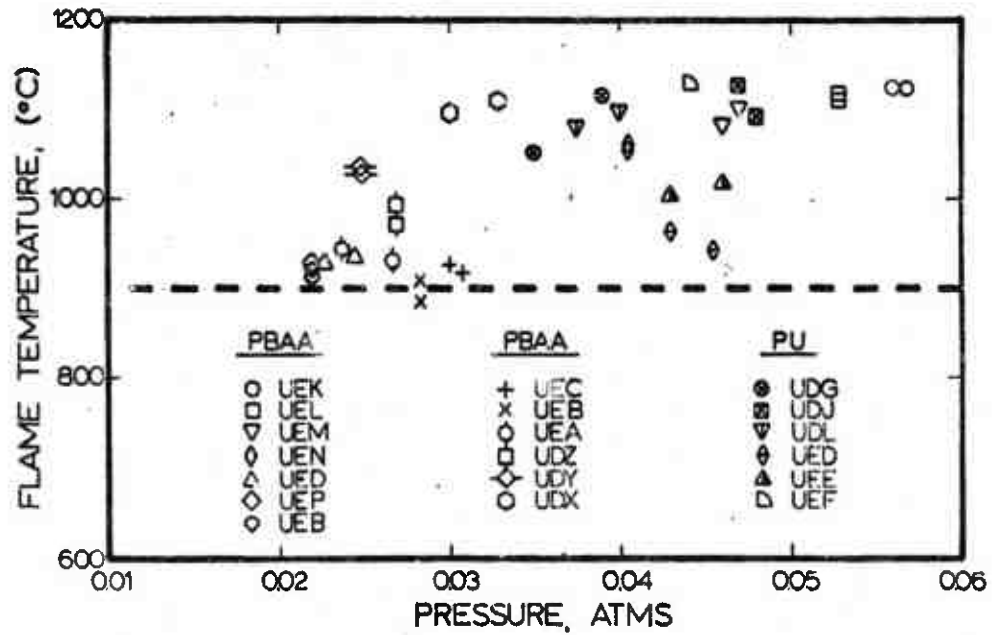


Figure 26. Uncorrected measured flame temperatures near P_{DL} for several propellants. The formulations represented a range from 75 to 85 percent AP. About half of the propellants contained 2 percent Harshaw CU-0202P catalyst.

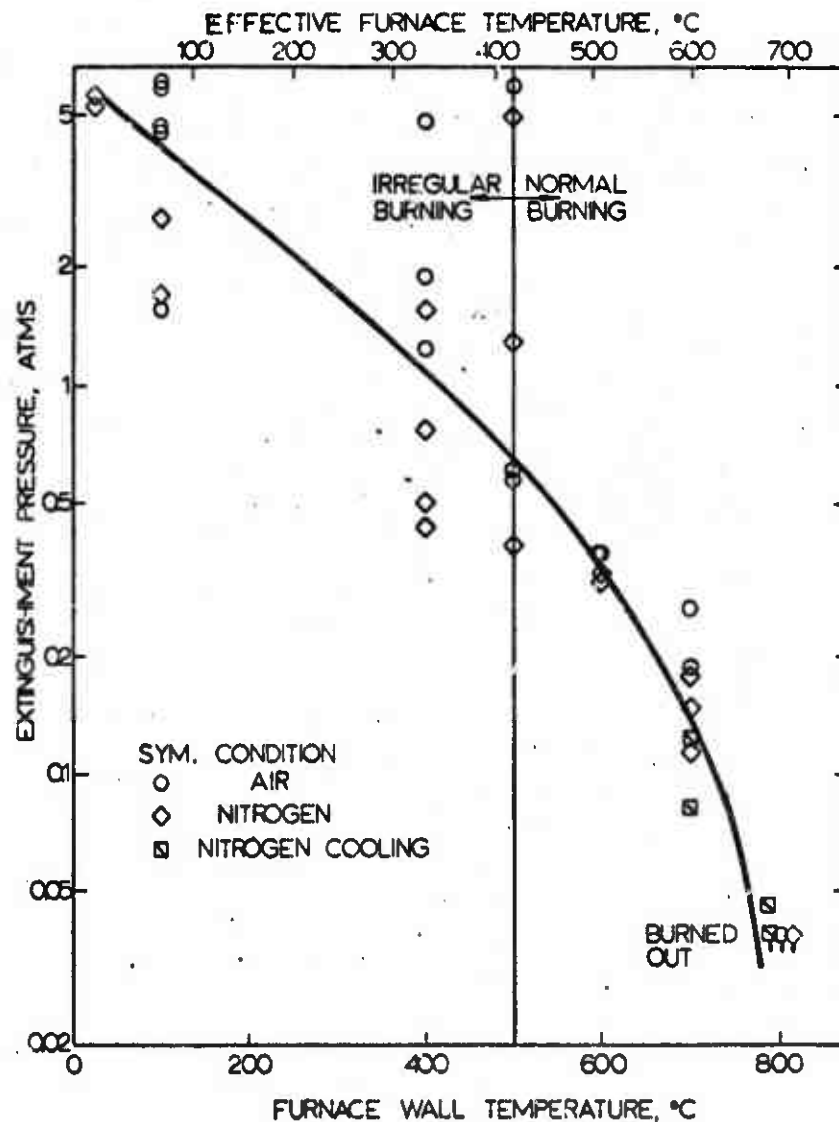


Figure 27. The extinguishment pressures for the Thiokol fluorocarbon-fueled TPF-1006 propellant strands when subjected to thermal radiation. The depressurization rate was 0.075 sec^{-1} . Where indicated, nitrogen flow was past the unburning surface of the strands to insure that the strand temperature was not increased by the radiant flux.

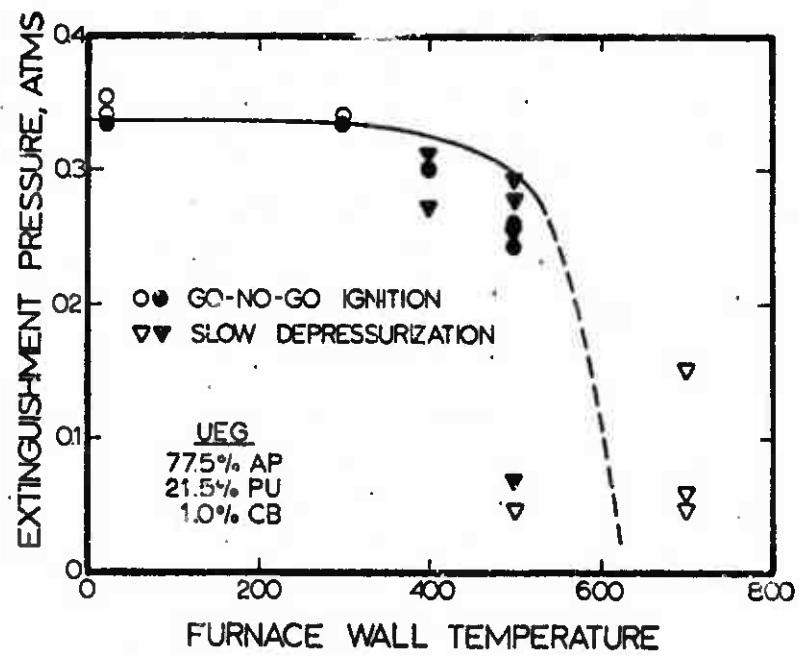


Figure 28. Extinguishment pressure for a polyurethane propellant when subjected to thermal radiation. The effective furnace temperatures are the same as indicated for Figure 27. For those tests indicated by triangles the depressurization rate was 0.075 sec⁻¹.

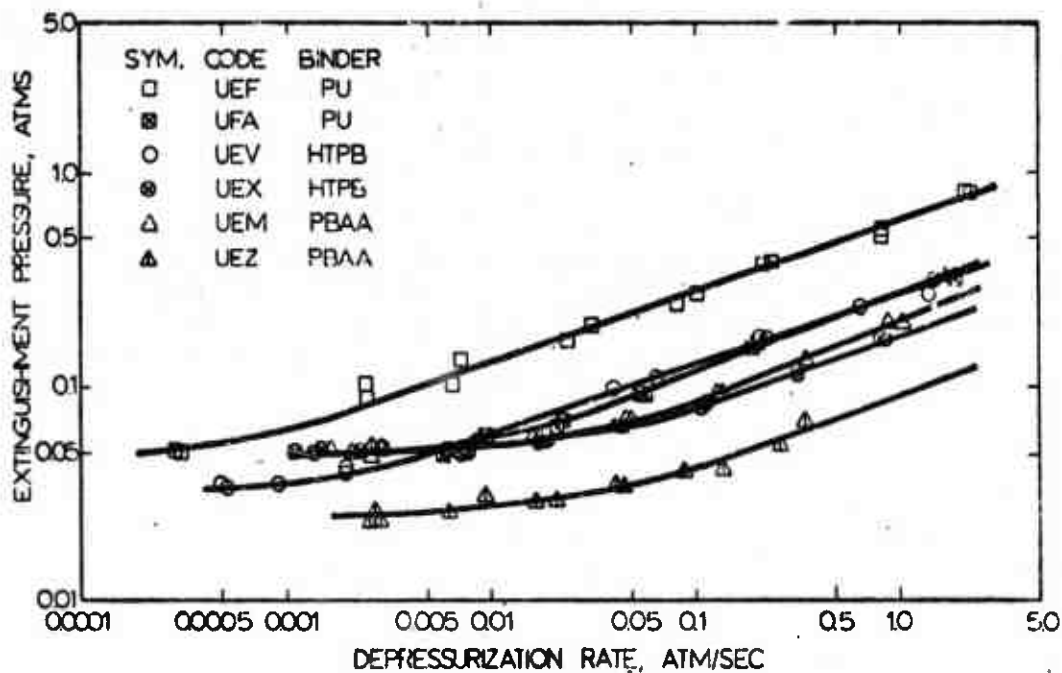


Figure 29. Extinguishment pressures are presented here for a series of related composite propellants as a function of the depressurization rate. All propellants contained 80 percent AP and 1 percent carbon black dispersed in the indicated polymers. Propellants designated by a crossed symbol also contained 2 percent of Harshaw CU-0202P catalyst.

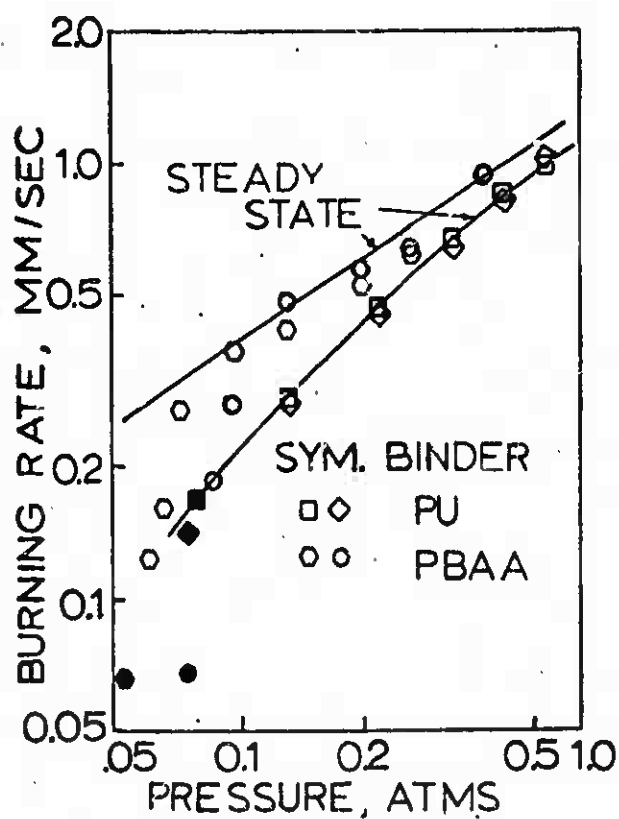


Figure 30. The measured transient burning rates at low pressure are presented here for two runs each employing the UEN and UEG propellants. The depressurization rate was 0.075 sec^{-1} , and the filled symbols indicate the last measurable values before mass loss from the strands ceased. The steady-state line was derived from measurements at constant pressure. The UEN and UEG propellants contained the PBAA and PU (Estane) fuel binders; each contained 77.5 percent AP.

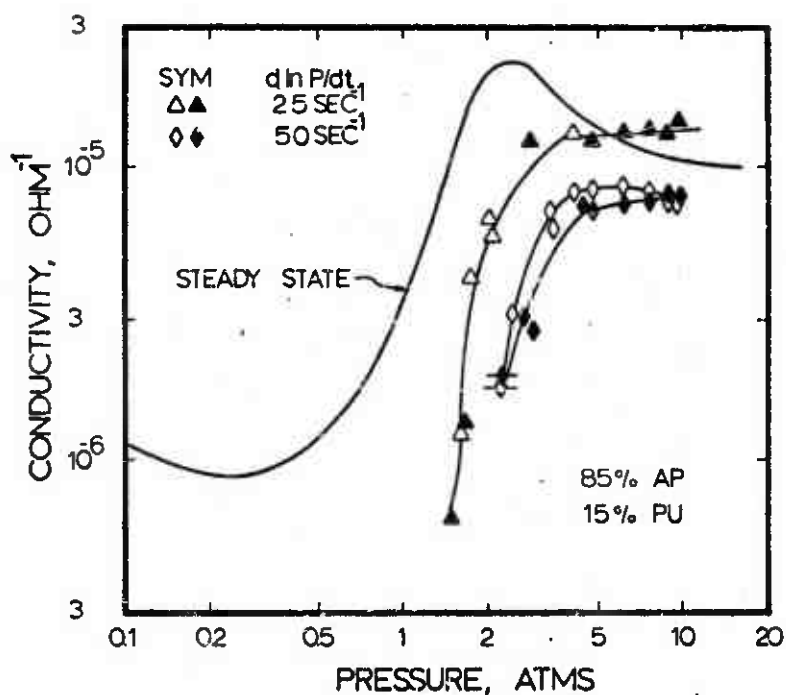


Figure 31. Measured, transient conductivity during depressurization of a polyurethane propellant. Deviation from the steady-state type of response was assumed to be due to deviation from equilibrium of the surface conditions. The initial conductivities at high pressures differed from the steady-state values because of variation in sample size.

APPENDIX B

REFERENCES

1. Baer, A. D., and Ryan, N. W. "Evaluation of Thermal-ignition Models from Hot-wire Ignition Tests," *Combustion and Flame*, 15 (1970), 9-22.
2. Baer, A. D., and Ryan, N. W. "Characterization of Solid Propellant Reactions from Hot-wire Ignition Data," Western States Section, The Combustion Institute, Paper 68-36, October, 1968.
3. Baer, A. D., and Ryan, N. W. "Ignition of Composite Propellants by Low radiant Fluxes," *AIAA Journal*, 3 (1965), 884-889.
4. Keller, J. A., Baer, A. D., and Ryan, N. W. "Ignition of Ammonium Perchlorate Composite Propellants by Convective Heating," *AIAA Journal*, 4 (1966), 1358-1365.
5. Keller, J. A., Baer, A. D., and Ryan, N. W. "The Ignition of Composite Solid Propellants by Hot Gases," *Pyrodynamics*, 3 (1965), 1-13.
6. Richardson, C. P., Baer, A. D., and Ryan, N. W. "An Effect of Gas Temperature on the Ignition of Composite Propellants," *Sixth ICRPG Combustion Conference, I* (CPIA Pub. No. 192: 1969), 389-397.
7. Wong, T. L., and Ryan, N. W. "Non-Acoustic Combustion Instability of Solid Propellants," Air Force Technical Report under Grants AF-AFOSR 446-67 and 69-1656 (1972).
8. Mantyla, R. G., and Ryan, N. W., "Combustion Instability in a Radial Burner," Air Force Technical Report under Grant AF-AFOSR 69-1656 (1972).
9. Oberg, C. L., Ryan, N. W., and Baer, A. D. "A Study of T-Burner Behavior," *AIAA Journal*, 6 (1968), 1131-1137.
10. Sipowicz, W. W., "Combustion Instability in a Gas-Fired T-Burner," Air Force Technical Report under Grant AF-AFOSR 69-1656 (1972).
11. Sipowicz, W. W., Ryan, N. W., and Baer, A. D. "Combustion-driven Acoustic Oscillations in a Gas-fired Burner," *Thirteenth Symposium (International) on Combustion*. Pittsburgh, Pennsylvania: The Combustion Institute, 1971. pp. 559-564.
12. Ryan, N. W., Sipowicz, W. W., and Baer, A. D., "Combustion-driven Oscillations in a Gas-fired T-Burner," *Sixth ICRPG Combustion Conference, I* (CPIA Pub. No. 192; 1969), 461-466.
13. Muhlfeith, C. M., Baer, A. D., and Ryan, N. W. "The Response of a Burning Solid Propellant Surface to Thermal Radiation." AFOSR Scientific Report No. TR-71-2664, AD-736049 (1971).

14. Muhlfeith, C. M., Baer, A. D., and Ryan, N. W. "The Direct Measurement of the Radiant Heat Flux Response Functions of Solid Propellants," *Eighth JANNAF Combustion Meeting, I* (CPIA Pub. No. 220; 1971), 259-275.
15. Muhlfeith, C. M., Baer, A. D., and Ryan, N. W. "Propellant Combustion Instability as Measured by Combustion Recoil," *AIAA Journal*, 10 (1972), 1280-1285.
16. Bestgen, R. F., and Wright, W. E., "A Study of the Effects of Electric Fields on Solid Propellant Burning Rates, AIAA Paper No. 71-174, AIAA Ninth Aerospace Sciences Meeting, January 1971.
17. Schulz, E. M., Baer, A. D., and Ryan, N. W. "Spectra and Temperature of Propellant Flames During Depressurization," *AIAA Journal*, 9 (1971), 869-875.
18. Chien, W. P., "Solid Propellant Flame Temperatures During Depressurization," M. S. Thesis, Department of Chemical Engineering, University of Utah, Salt Lake City, Utah October, 1970.
19. Baer, A. D., Chien, W. P., and Ryan, N. W. "Transient Flame Temperatures and Depressurization Extinguishment of Composite Propellant Strands," *Eighth JANNAF Combustion Meeting, I* (CPIA Pub. No. 220; 1971), 441-454.
20. Park, C. P., Ryan, N. W., and Baer, A. D., "Extinguishment of Composite Propellants at Low Pressures," AIAA Paper No. 73-175, AIAA Eleventh Aerospace Sciences Meeting (1973).